Environmental Science & Technology

Article

pubs.acs.org/est

Identification of Thyroid Hormone Disruptors among HO-PBDEs: *In Vitro* Investigations and Coregulator Involved Simulations

Qinchang Chen,[†] Xiaoxiang Wang,[†,‡] Wei Shi,[*,†] Hongxia Yu,[*,†] Xiaowei Zhang,[†] and John P. Giesy[†,§,∥,⊥]

[†]State Key Laboratory of Pollution Control and Resources Reuse, School of the Environment, Nanjing University, Nanjing 210023, PR China

[‡]Multiphase Chemistry Department, Max Planck Institute for Chemistry, 55128 Mainz, Germany

[§]Department of Veterinary Biomedical Sciences and Toxicology Centre, University of Saskatchewan, Saskatoon, Saskatchewan S7N 5B4, Canada

[∥]Department of Zoology and Center for Integrative Toxicology, Michigan State University, East Lansing, Michigan 48824, United States

[⊥]School of Biological Sciences, University of Hong Kong, Hong Kong, SAR, China

Supporting Information

ABSTRACT: Some hydroxylated polybrominated diphenyl ethers (HO-PBDEs), that have been widely detected in the environment and tissues of humans and wildlife, bind to thyroid hormone (TH) receptor (TR) and can disrupt functioning of systems modulated by the TR. However, mechanisms of TH disrupting effects are still equivocal. Here, disruption of functions of TH modulated pathways by HO-PBDEs was evaluated by assays of competitive binding, coactivator recruitment, and proliferation of GH3 cells. *In silico* simulations considering effects of coregulators were carried out to investigate molecular mechanisms and to predict potencies for disrupting functions of the TH. Some HO-PBDEs were able to bind to TR with moderate affinities but were not agonists. In GH3 proliferation assays, 13 out of 16 HO-PBDEs were antagonists for the TH. *In silico* simulations of molecular dynamics revealed that coregulators were essential for identification of TH disruptors. Among HO-PBDEs, binding of passive antagonists induced repositioning of H12, blocking AF-2 (transactivation function 2) and preventing recruitment of the coactivator. Binding of active antagonists exposed the coregulator binding site, which tended to bind to the corepressor rather than the coactivator. By considering both passive and active antagonisms, anti-TH potencies of HO-PBDEs could be predicted from free energy of binding.

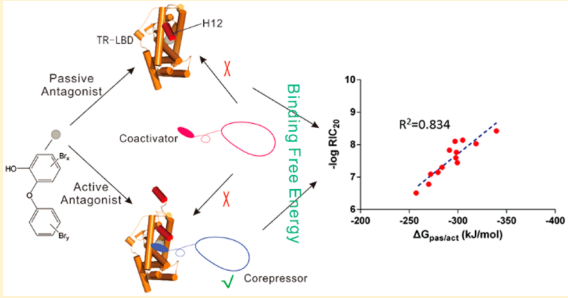

INTRODUCTION

Hydroxylated polybrominated diphenyl ethers (HO-PBDEs), which can be natural or transformation products of synthetic compounds,[1,2] are ubiquitous in soil, water, and sediments[3,4] and detectable in fish, birds, and mammals, including humans.[5−7] Greater concentrations of HO-PBDEs have been found in neonates than their corresponding mothers, which suggested potential for adverse effects on neurodevelopment.[7] Due to their structural similarities with endogenous thyroid hormones (THs, e.g. 3,5,3′-triiodothyronine, T_3), HO-PBDEs have already raised concern due to their potential disruption of functioning of TH, which is essential for early development of mammals. *In vitro* assays have shown that HO-PBDEs can inhibit binding of T_3 to TH receptor (TR)[8,9] and are more toxic than PBDEs.[10,11] Results of a reporter gene assay have indicated that 4-HO-BDE-90 and 4′-HO-BDE-49 are antagonists of the TR.[12] However, in a two-hybrid yeast assay, they were all determined to be agonists of the TRβ.[13] Divergence in results of studies reveals the necessity of structural and mechanical interpretation of potential for effects on functions of TR.

Despite limited information on toxicity caused by disruption of TH homeostasis, little was known about mechanisms by which HO-PBDEs interfere with the TR. Quantitative structure−activity relationship (QSAR) models based on molecular docking have been developed.[13,14] A robust QSAR model to predict binding of HO-PBDEs to TR, based on hydrogen bonding and electrostatic interactions as characteristic of interactions between HO-PBDEs and TR, has been developed.[13] However, QSAR models are "ligand-based", and molecular descriptors do not integrate all of the possible interactions between ligands and receptors.[15] This then results in less precise predictions, because predictions based on docking of ligands alone is limited by molecular flexibility.[16]

Received: April 25, 2016
Revised: October 12, 2016
Accepted: October 13, 2016
Published: October 14, 2016

DOI: 10.1021/acs.est.6b02029
Environ. Sci. Technol. 2016, 50, 12429−12438

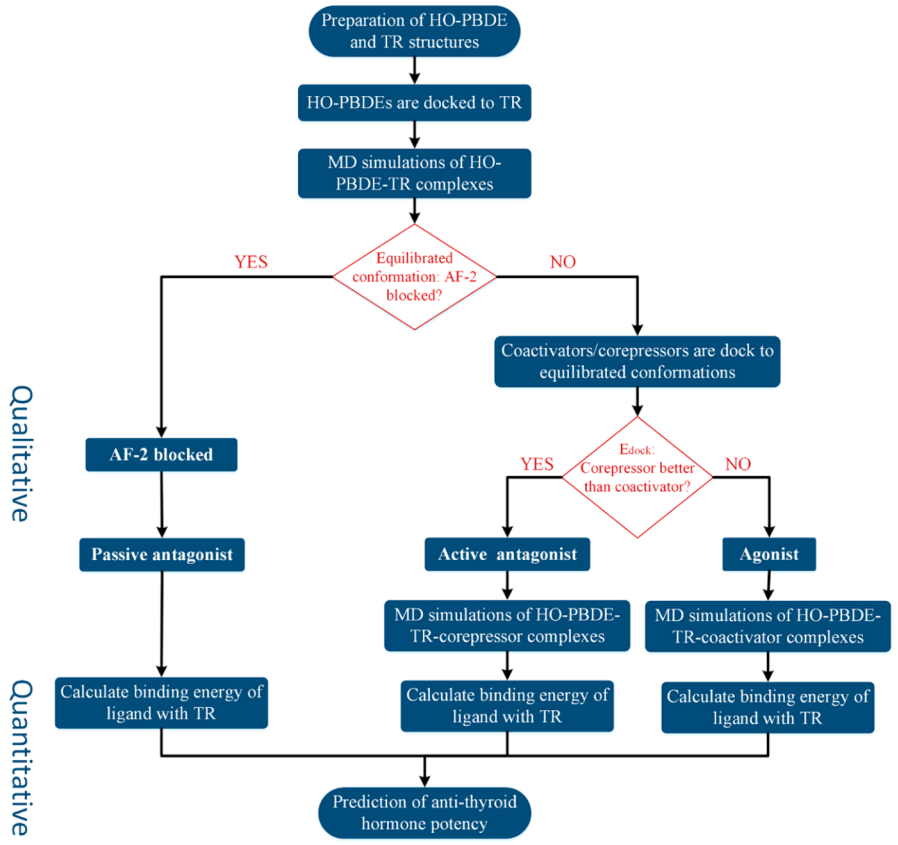

Figure 1. Protocol for prediction of thyroid hormone disrupting effect of HO-PBDEs.

Simulations based on molecular dynamics (MD) relax the ligand−receptor complex and are recommended for more comprehensive simulations.[17] However, few MD simulations have been performed on TR, and seldom have quantitative descriptors been used to make predictions.

As a member of the ligand-dependent nuclear receptor (NR) superfamily, functions of TR are associated with coregulators (coactivator and corepressor). TR contains a transactivation domain, called activation function 2 (AF-2), in the ligand binding domain (LBD),[18,19] which is activated upon binding of agonists that are capable of recruitment of the coactivator.[20] Binding of T_3 induces a series of conformational changes in the LBD, including repositioning of helix 12 (H12), which activates AF-2 and promotes recruitment of the coactivator, followed by transactivation of target genes. The corepressor binds to a surface partially overlapping AF-2 and represses transcription of target genes modulated by TH, even when no ligand is bound.[21,22] Binding of antagonists enhances recruitment of the corepressor or blocks binding of the coactivator.[23,24] Upon coregulator interactions, ligands inhibiting TH function can be classified as a "passive antagonist" if it blocks binding of the coactivator and the relative transactivation or an "active antagonist" which enhances recruitment of the corepressor.[25] Therefore, coregulators are essential for functioning of the TR, which can be used as a factor for classification of TH disruptors. However, to the best of our knowledge, no research identifying disruptors of TH have used coregulators.

It has been challenging to quantitatively predict relative endocrine disrupting potencies. A MD study using settling time, the simulation time needed to stably reposition, of H12 as a predictor of antiandrogenic potency has been conducted.[26] However, both stable H12 and settling time were subjectively estimated, which were not sufficient for making quantitative predictions. In fact, settling of H12 and equilibrium of the receptor can be described in terms of free energy.[27] Binding free energy is a quantified term for interaction strength between molecules, such as ligand−receptor and protein−protein.[28] Results of previous studies have revealed that binding free energy can be used to predict binding affinity and kinase inhibiting activity.[29,30] Binding free energy gave a good correlation with biological activities of B-RAF kinase inhibitors.[30] Although binding energy was also used to compare NR-mediated endocrine disrupting potencies, it was usually based on molecular docking.[31] Accordingly, binding free energy calculated from MD simulations should be a good quantitative predictor for TH disruptors.

In the current study, a combination of *in vitro* assays and *in silico* simulations was used to investigate TH disrupting effects of HO-PBDEs. TH disrupting activities of HO-PBDEs were detected by protein- and cell-based *in vitro* assays. MD simulations, based on effects of coregulators, were performed to determine the mechanism of functioning of the TR. For the first time, TH disrupting chemicals were identified by computational simulations based on coregulator associated mechanisms. Finally, free energies of binding were calculated to quantitatively predict antagonistic effects of HO-PBDEs (Figure 1). This methodology can be used for screening of other potential endocrine disrupting chemicals, and binding free energy can be used as a descriptor in QSAR models to predict binding to the TR.

DOI: 10.1021/acs.est.6b02029
Environ. Sci. Technol. 2016, 50, 12429−12438

MATERIALS AND METHODS

Materials. Recombinant human TRα- and TRβ-LBD (GST-tagged) were purchased from Life Technology (Carlsbad, CA, USA). 3,5,3′-Triiodothyronine (T_3; 99% purity) was purchased from Fitzgerald Industries International Inc. (Concord, MA, USA). Sixteen HO-PBDEs were selected for the present investigation (see Supporting Information, Figure S1). Twelve of these HO-PBDE congeners (>98% pure) were synthesized in the Department of Biology and Chemistry of City University of Hong Kong following previously published methods;[32] the four other congeners (50 μg/mL or 10 μg/mL in acetonitrile) were purchased from AccuStandard (New Haven, CT, USA). Stock solutions of ligands, including HO-PBDEs and T_3, were prepared in dimethyl sulfoxide (DMSO; Sigma, St. Louis, MO, USA) and stored at −20 °C. The four HO-PBDEs (4-HO-BDE-188, 4′-HO-BDE-101, 6′-HO-BDE-99, and 6-HO-BDE-157) from AccuStandard were not tested in competitive binding assays because sufficiently high concentrations were unavailable.

Competitive Binding Assay. The competitive binding assay was based on fluorescein-labeled T_3 (F-T_3) that was developed and employed as a probe to assess potencies of binding between ligands and TR-LBDs. Methods of F-T_3 synthesis and characterization have been described previously[8] and are detailed in the Supporting Information. The probe is able to bind to TR-LBD with high affinity, while binding of a ligand with the LBD displaces F-T_3 and reduces the magnitude of fluorescence polarization (millipolarization, mP). A detailed description was given in the Supporting Information. Quench control experiments were not included, but a series of structurally related compounds were studied, which was useful in the absence of quench data.

Coactivator Recruitment Assay. Fluorescein-SRC2-2 Coactivator Peptide (Life Technology, Carlsbad, CA, USA) was introduced as a probe to assess potencies of HO-PBDEs and T_3 as agonists of the TR. Upon binding of the ligand, an agonist is able to induce conformational changes of the TR-LBD and recruitment of the coactivator peptide, resulting in an increase in polarization. The assay was detailed in the Supporting Information.

GH3 Cell Proliferation Assay. The rat pituitary tumor cell line GH3 was purchased from China Infrastructure of Cell Line Resources (Beijing, China) and cultured as recommended. Details for cell culture and experimental testing were described in the Supporting Information. The GH3 cell line has been reported to express high level TRs and be responsive to THs by proliferating.[33] HO-PBDEs were assessed for potency as TR agonists or antagonists in the absence or presence of 0.5 nM T_3 (median effective concentration of T_3), respectively. In each assay, the final DMSO content was kept below 0.1% (v/v) to avoid cytotoxicity.

***In Silico* Simulations.** Structures of ligands and apo TRs for MD simulations were prepared according to previously reported methods[26,34] which are described in more detail in the Supporting Information. Ligands were docked into apo TRs by SYBYL 7.3 (Tripos Inc., St. Louis, MO, USA), and MD simulations were performed using the GROMACS 4.5 package,[35,36] which were detailed in the Supporting Information.

Three equilibrated conformations (see the Supporting Information) were extracted for every receptor exposing coregulator binding surface. The detail description of protein docking was given in the Supporting Information. One of the 3 conformations was selected to perform MD simulations again for the ligand−receptor−corepressor complexes.

Trajectories obtained from MD simulations were used for binding free energy calculations using the molecular mechanics Poisson−Boltzmann surface area (MM-PBSA) method, which was detailed in the Supporting Information. All calculations of MM-PBSA were performed by use of the g_mmpbsa package[28] developed form GROMACS and APBS[37] programs.

Data Analysis. Competition curves for various ligands were fitted by means of dose−response inhibition using GraphPad Prism Version 5.01 (GraphPad Software Inc., San Diego, CA, USA). Results of the competitive binding assay, coactivator recruitment assay, and GH3 proliferation assay were expressed as the mean ± standard deviations of at least three independent experiments. One-way analysis of variance (ANOVA) followed by Dunnett's multiple comparisons were performed to compare each treatment, with p-values ≤0.05 considered significant. Concentrations associated with IC_{50} (median inhibition) and RIC_{20} (20% inhibition) were derived from the dose−response curves (eq 1)

$$Y = \text{Bottom} + \frac{\text{Top} - \text{Bottom}}{1 + 10^{X - \log IC_{\text{Median}}}} \quad (1)$$

where IC_{Median} is the concentration of ligand that gives a response half way between Bottom and Top. GROMACS 4.5 was also used to analyze results of the MD simulations. Root-mean-square deviation (RMSD) of H12 was calculated for all succeeding frames. The backbone was set as a reference structure for alignment. The combined binding free energy $\Delta G_{\text{pas/act}}$ combining binding free energies of passive and active antagonists was calculated (eq 2)

$$\Delta G_{\text{pas/act}} = \Delta G_{\alpha} + \Delta G_{\beta} \quad (2)$$

where ΔG_{α} is $\Delta G_{\text{lig-rTR}\alpha}$ for passive antagonists or $\Delta G_{\text{lig-rTR}\alpha/\text{cor}}$ for active antagonists, and ΔG_{β} is $\Delta G_{\text{lig-rTR}\beta}$ for passive antagonists or $\Delta G_{\text{lig-rTR}\beta/\text{cor}}$ for active antagonists. Here $\Delta G_{\text{lig-rTR}\alpha}/\Delta G_{\text{lig-rTR}\beta}$ and $\Delta G_{\text{lig-rTR}\alpha/\text{cor}}/\Delta G_{\text{lig-rTR}\beta/\text{cor}}$ were ligand−receptor binding free energies.

RESULTS AND DISCUSSION

TH Disrupting Effects Tested by Recombinant TR-LBD. As an endogenous TH used as a positive control, in the competitive binding assay, T_3 exhibited affinity for LBDs of both human TRα and TRβ. A decrease in polarization was observed, and IC_{50}s of 3.25×10^{-7} M and 2.48×10^{-7} M for T_3 binding to TRα and TRβ, respectively (Figure S3 A, B and Table S1), were obtained, which were similar and consistent with results of a previous study.[9] It might be due to the high level of receptor needed for fluorescence polarization assays[38,39] that the binding curves showed very steep slopes, and the derived IC_{50}s were 3 to 4 orders of magnitude greater than the reported binding affinity by use of the ^{123}I-T_3 competitive binding assay.[8] Therefore, the results were still helpful for determining rank-order binding affinities. Based on competition curves (Figure S3A), 2-HO-BDE-123, 3-HO-BDE-100, and 6-HO-BDE-137 exhibited detectable affinities to the LBD of TRα. IC_{50} values ranged from 1.38×10^{-4} M to 1.87×10^{-4} M (Table S1), which were hundreds of times greater than T3. 3-HO-BDE-100 and 6-HO-BDE-137 exhibited detectable affinities for the LBD of TRβ (Figure S3B), which were 5.6- and 60-fold greater than those for TRα, respectively. All other

DOI: 10.1021/acs.est.6b02029
Environ. Sci. Technol. 2016, 50, 12429−12438

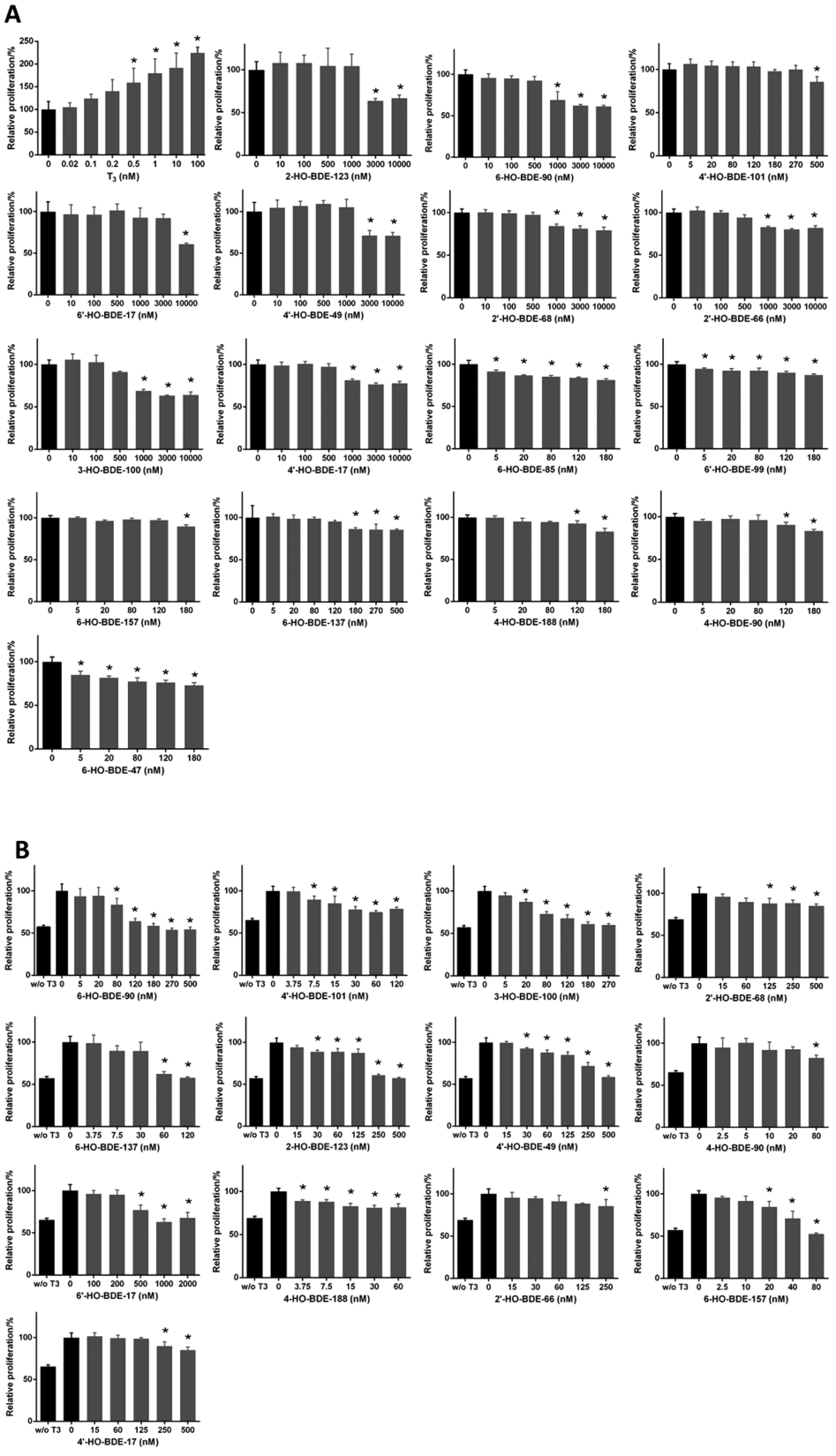

Figure 2. Results of GH3 proliferation assays. (A) Proliferation and cytotoxicities of GH3 cells exposed to various concentrations of chemicals. Relative proliferation of solvent (DMSO) controls are defined 100%. (B) Inhibition of HO-PBDEs on proliferation of theh GH3 cell line induced by 0.5 nM T_3. Concentrations of HO-PBDEs are no greater than the noncytotoxic concentrations. Relative proliferation of solvent controls (0.5 nM T_3 without HO-PBDEs) are defined as 100%. The column labeled "w/o T3" is the baseline control without T3 and testing chemical. The error bar refers to the standard deviation (SD) of at least three independent experiments. *$p < 0.05$ compare with solvent control.

DOI: 10.1021/acs.est.6b02029
Environ. Sci. Technol. 2016, 50, 12429−12438

Table 1. Anti-TH Potencies of HO-PBDEs on the GH3 Cell Line and Relative *in Silico* Parameters[a]

			TRα (kJ/mol)			TRβ (kJ/mol)			combined (kJ/mol)	
chemical	noncytotoxic concn	$-\log RIC_{20}$	$\Delta G_{lig-rTR\alpha}$	$\Delta G_{lig-rTR\alpha/cor}$	$\Delta G_{cor-rTR\alpha}$	$\Delta G_{lig-rTR\beta}$	$\Delta G_{lig-rTR\beta/cor}$	$\Delta G_{cor-rTR\beta}$	$\Delta G_{sum,cor-rTR}$	$\Delta G_{pas/act}$
4-HO-BDE-188	8×10^{-8} M	8.42	−175.2	−170.1	−132	−169.7	−169.4	−87.0	−344.9	−339.5
3-HO-BDE-100	5×10^{-7} M	7.83	−139.7	−150.7	−42.6	−137.5	−140.6	−81.6	−277.2	−291.3
4′-HO-BDE-101	2.7×10^{-7} M	8.11	−150.7	−150.6	−109.2	−150.6	−146.5	−64.0	−301.3	−297.1
6-HO-BDE-157	1.2×10^{-7} M	8.14	−149.5	−150.6	−9.89	−156.8	−154.3	−46.1	−306.3	−304.9
6-HO-BDE-90	5×10^{-7} M	7.76	−143.3	−145.6	−71.9	−151.7	−152.9	10.0	−295.1	−298.5
4′-HO-BDE-49	1×10^{-6} M	7.30	−141.5	−142.1	−34.0	−141.4	−141.6	−58.9	−282.9	−283.7
2′-OH-BDE-66	5×10^{-7} M	7.09	−142.5	−139.0	−31.7	−136.4	−133.1	−32.5	−278.8	−272.1
6′-HO-BDE-17	3×10^{-6} M	6.78	−128.1	−136.4	−59.8	−135.0	−133.7	−35.2	−263.1	−270.1
2′-OH-BDE-68	5×10^{-7} M	7.15	−136.2	−132.1	−25.8	−142.5	−147.3	−56.0	−278.7	−279.5
4′-OH-BDE-17	5×10^{-7} M	6.51	−126.9	−126.2	−70.5	−131.4	−131.0	−67.8	−258.3	−257.2
6-HO-BDE-137	1.2×10^{-7} M	8.03	−161.3	−156.3	−76.1	−162.2			−323.5	−318.6
2-HO-BDE-123	1×10^{-6} M	7.44	−152.5	−149.8	−60.2	−149.5			−302.0	−299.3
4-HO-BDE-90	8×10^{-8} M	7.59	−147.8	−151.8	−37.1	−146.2			−293.9	−297.9
6-HO-BDE-47	$<5 \times 10^{-9}$ M		−145.3	−140.8	−53.0	−135.4	−137.3			
6-HO-BDE-85	$<5 \times 10^{-9}$ M		−138.3			−150.8	−151.3	−72.9	−289.1	−289.6
6′-HO-BDE-99	$<5 \times 10^{-9}$ M		−139.1	−137.7	−81.4	−144.3	−148.5	−55.3	−283.4	−286.2
unbound					−26.7			−50.7		

[a]Noncytotoxic concentration: The highest concentration in Figure 2A that does not show cytotoxicity. $-\log RIC_{20}$: negative logarithm of the concentration (mol/L) showing 20% inhibition of GH3 proliferation induced by 0.5 nM T3. $\Delta G_{lig-rTR\alpha}/\Delta G_{lig-rTR\beta}$: binding free energies of ligand with TRα/TRβ-LBD without the corepressor. $\Delta G_{lig-rTR\alpha/cor}/\Delta G_{lig-rTR\beta/cor}$: binding free energies of ligand with TRα/TRβ-LBD complex with the corepressor. $\Delta G_{cor-rTR\alpha}/\Delta G_{cor-rTR\beta}$: binding free energies of the corepressor peptide with TRα/TRβ-LBD. $\Delta G_{sum,lig-rTR}$: combined binding free energy of $\Delta G_{lig-rTR\alpha}$ and $\Delta G_{lig-rTR\beta}$. $\Delta G_{pas/act}$: combined binding free energy of passive and active antagonists.

HO-PBDEs exhibited weak binding to the TR, which could not be observed at a concentration between 4.0×10^{-7} and 1.6×10^{-4} M.

Results of the human TRα coactivator recruitment assay demonstrated that adding of T_3 significantly ($p < 0.05$) increased relative polarization by 34.8% and 30.0% in lesser (1.0×10^{-6} M) and greater (4.0×10^{-6} M) concentrations, respectively (Figure S3C). Greater polarization was due to recruitment of the SRC2-2 peptide by T_3-bound TRα. However, no significantly ($p < 0.05$) greater polarization was observed for the HO-PBDEs with potent binding affinities. Results of the TRβ coactivator recruitment assay were similar to those for the TRα. These results indicated that HO-PBDEs might not be agonists of the TR or that the agonistic effect on TR was too slight to be detected. In fact, some HO-PBDEs, including 3-HO-BDE-100 have been determined to be antagonists of the TR.[9,12]

TH Disrupting Effects Determined by the GH3 Cell Line. With increasing doses of T_3 from 0.02 to 100 nM in the serum-free medium, GH3 cell proliferation increased (Figure 2A, up left). Maximal proliferation of about 2-fold was observed at 100 nM, and the half maximal effect (EC_{50}) was 0.5 nM. No promoted GH3 cell proliferation was observed for tested HO-PBDEs (Figure 2A), which indicated that all 16 HO-PBDEs were not TH agonists. Instead, due to cytotoxicity, proliferation was significantly ($p < 0.05$) less, compared to solvent control in a dose-dependent manner. Noncytotoxic concentrations of most of the tested HO-PBDEs ranged from 80 to 3000 nM (Table 1), while cytotoxicities of 6-HO-BDE-47, 6-HO-BDE-85, and 6′-HO-BDE-99 were observed at a concentration of 5 nM. Thus, their cytotoxicities were more than 16-fold greater than the greatest cytotoxicity (noncytotoxic concentration = 80 nM) observed for the other 13 compounds. It has been previously reported that 6-HO-BDE-47 and 6-HO-BDE-85 caused significant cytotoxicity to rat hepatoma cells,[40] which makes it difficult to eliminate effects of cytotoxicity during anti-TH assays. Therefore, concentrations of HO-PBDEs were kept within the noncytotoxic concentrations (Table 1) in the following tests for anti-TH potency, and 6-HO-BDE-47, 6-HO-BDE-85, and 6′-HO-BDE-99 were not included. However, from a risk assessment perspective, this means that effects on the TH would be unlikely to be the critical mode of toxic action.

Tested HO-PBDEs significantly ($p < 0.05$) inhibited proliferation of GH3 cells stimulated by 0.5 nM T_3, compared to solvent control (Figure 2B). Since inhibition of proliferation did not go beyond the baseline control (no T_3, no HO-PBDE), the results suggested that these HO-PBDEs are TR antagonists. 4-HO-BDE-188 and 4′-HO-BDE-101 are the most effective inhibitors that significantly ($p < 0.05$) reduced proliferation, at concentrations of 3.75 or 7.5 nM, respectively. 4′-HO-BDE-17 and 6′-HO-BDE-17 were the weakest antagonists, which inhibited proliferation of GH3 cells at concentrations of 250 or 500 nM, respectively. Potencies of HO-PBDEs as antagonists, reported as the $-\log RIC_{20}$ (Table 1), ranged from 6.51 to 8.42. These results are consistent with those of a previous study in which GH3 cells were used.[9] 3-HO-BDE-100 and 2-HO-BDE-123 were potent competitors in the competitive binding assays, with binding affinities of 3-HO-BDE-100 greater than 2-HO-BDE-123, which were consistent with the derived anti-TH potencies. While the 6-HO-BDE-90, which was a less potent competitor, effects of which could not be observed in competitive binding assays, showed relatively great anti-TH potency in GH3 cell proliferation assays, indicating the importance of functioning mechanisms of TR. HO-PBDEs with more Br atoms tended to exhibit greater antagonistic potencies than lesser brominated HO-PBDEs. For example, heptabrominated 4-HO-BDE-188 ($-\log RIC_{20} = 8.42$) and hexabrominated 6-HO-BDE-157 ($-\log RIC_{20} = 8.14$) exhibited much greater potency than tribrominated 4′-HO-BDE-17 ($-\log RIC_{20} = 6.51$) and 6′-HO-BDE-17 ($-\log RIC_{20} = 6.78$). Results also indicated that HO-PBDEs are more potent anti-TH disruptors

DOI: 10.1021/acs.est.6b02029
Environ. Sci. Technol. 2016, 50, 12429−12438

than PBDEs ($-\log RIC_{20} < 5$)[41] and BPA ($-\log RIC_{20} = 6$),[42] which are known TR antagonists.

Repositioning of H12 and Binding Free Energy. During MD simulations, ligand−receptor complexes experienced conformational dynamics, and conformations of TR, especially positions of H12s, significantly changed (see the Supporting Information), which was consistent with a previous study of AR.[26] Binding free energy could be used for prediction of binding affinities with TR. Lesser binding free energy might indicate greater binding affinity. HO-PBDEs with greater affinities for binding with human TRα in the competitive binding assays exhibited lesser binding free energy (Table S1). However, binding of the coregulator to the ligand−receptor complex influenced the binding affinity. For example, 6′-HO-BDE-17, which bound rat TR with high binding free energy, lowered the binding free energy with TRα when complexed with the corepressor and exhibited greater binding affinity (Table 1). These results revealed that more attention should be paid to the mechanism, especially the interaction with coregulators.

Passive Antagonists. Snapshots of equilibrated conformations (see the Supporting Information) were extracted to investigate the reposition of H12. 3-HO-BDE-100-hTRα-H12 (H12 of 3-HO-BDE-100-bound human TRα), 2-HO-BDE-123-hTRβ-H12, 6-HO-BDE-85-rTRα-H12, 2-HO-BDE-123-rTRβ-H12, 4-HO-BDE-90-rTRβ-H12, and 6-HO-BDE-137-rTRβ-H12 were found to block AF-2 (Figure 3B and Figure S6). For example, 3-HO-BDE-100-hTRα-H12 positioned between residues V230, K234 and I248, K252, which were components of AF-2.[21] Distances between H12 and these residues are approximately 3 Å and could be as close as 2.2 Å, which indicated that AF-2 was partly blocked (Figure 3B). Blocking AF-2 prevents subsequent transactivation of a target gene, thus is defined as passive antagonism.[25,43] In the present study, 2-HO-BDE-123, 4-HO-BDE-90, and 6-HO-BDE-137 were determined to be antagonists of the TR in the GH3 proliferation assay. Therefore, these HO-PBDEs could be considered to be passive antagonists of TR. For T_3-bound human TRβ, AF-2 was exposed to the coregulators, so that coactivators were able to bind it (Figure 3A).

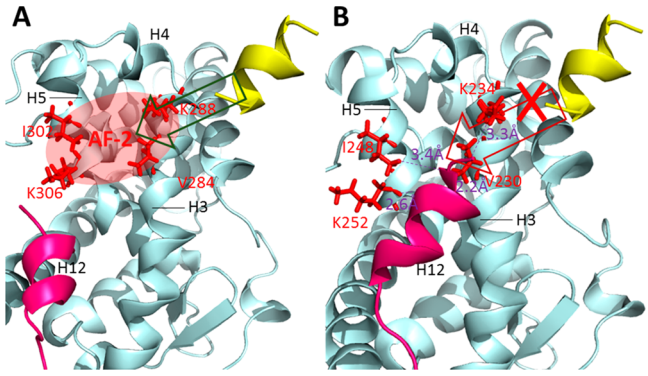

Figure 3. Close-up view of human TRα-/TRβ and coactivator peptides. H1 to H11 of the LBDs are shown in light blue; H3, H4, and H5 are labeled. H12s and coactivator peptides are colored hot pink and yellow, respectively. Residues V284, K288, I302, and K306 of TRβ (V230, K234, I248, and K252 for TRα), which are components of activation function 2 (AF-2), are labeled and colored red. (A) T_3-bound TRβ, the AF-2 (elliptical area in red) is suitable for binding of the coactivator. (B) 3-HO-BDE-100-bound TRα, AF-2 is partly occupied by stable H12, preventing recruitment of the coactivator. Distances between H12 and the 4 residues are labeled purple.

Active Antagonists. For those conformations whose AF-2 were exposed to coregulators, HO-PBDE-bound TRs tended to be more attractive to corepressors than coactivators. Most of the HO-PBDE-bound TRs bound to the corepressor with an E_{dock} value less than that of the coactivator except 6-HO-BDE-47-bound TRβ (Figure 4), which meant that corepressors were more selectively bound to them. For 2-HO-BDE-123-, 4′-HO-BDE-17-, 6-HO-BDE-157-, 6-HO-BDE-90-, and 6′-HO-BDE-99-bound TRα, as well as 4-HO-BDE-188-, 4′-HO-BDE-101-, 6-HO-BDE-90-, and 6-HO-BDE-157-bound TRβ, the deviation values were even less than that of unbound TRα and TRβ (about −20). Alternatively, both T_3-bound TRα and TRβ bound to coactivators with E_{dock} values less than that of the corepressor, which suggested that TRs bound to T_3 recruit coactivators rather than corepressors. It has been reported that T_3 induces recruitment of coactivators, while unbound TR is able to bind corepressors.[44] These results indicated that most of the HO-PBDEs selectively enhanced recruitment of corepressors rather than coactivators. Corepressor-bound TR is able to bind to relative genes and silence transactivation,[45] which was defined as active antagonism.[25] In the present study, HO-PBDEs causing selective binding of corepressors to TR were considered to be active antagonists.

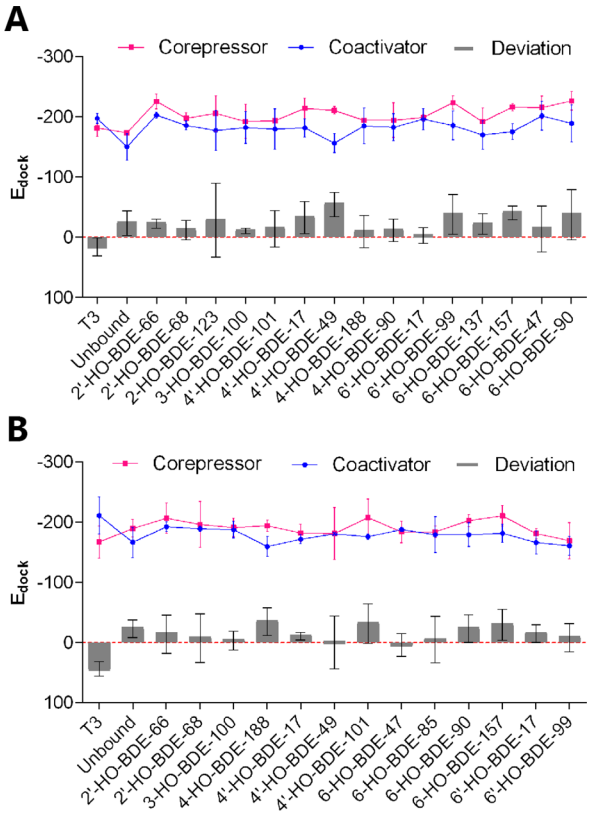

Figure 4. Docking score (E_{dock}) of the corepressor and the coactivator with rat TRα (A) and TRβ (B). Deviation is the difference of E_{dock} between the corepressor and the coactivator. The error bar refers to the standard deviation (SD) of three independent conformations.

When MD simulations with the corepressor on the corepressor binding site were performed, it was further demonstrated that most of the HO-PBDEs maintained or even strengthened interactions between the receptor and the

DOI: 10.1021/acs.est.6b02029
Environ. Sci. Technol. 2016, 50, 12429−12438

corepressor. Binding free energies for corepressors with TRα and TRβ ($\Delta G_{cor-rTR\alpha}$ and $\Delta G_{cor-rTR\beta}$, kJ/mol) of unbound TR were −26.7 and −50.7 kJ/mol, respectively (Table 1). For HO-PBDEs, values of $\Delta G_{cor-rTR\alpha}$ ranged from −9.89 (6-HO-BDE-157) to −132 (4-HO-BDE-188), and $\Delta G_{cor-rTR\beta}$ ranged from 10.0 (6-HO-BDE-90) to −87.0 (4-HO-BDE-188). Binding of 4-HO-BDE-188 reduced $\Delta G_{cor-rTR\alpha}$, which indicated strengthened interaction between the corepressor and TRα and further repression of transactivation. It has been reported that binding of TH to TR resulted in unbinding of the corepressor.[44] However, results presented here demonstrated that HO-PBDEs were able to bind to the ligand binding cavity of the TR and change the interaction between the corepressor and TR. In fact, some endocrine disrupting chemicals have been found to exert anti-TH activity by causing recruitment of corepressors. For example, enhanced interaction between TR and the corepressor was found to be caused by bisphenol A (BPA).[42] For the first time, our investigation demonstrates that HO-PBDEs enhance TR-corepressor interaction.

Essential Residues to TR-Corepressor Interaction. H12 is important in binding of coregulators to TR.[46] Deletion of H12 was reported to increase binding of the corepressor to unbound TR.[42] However, results of the present study revealed that H12 plays different roles in different situations. For passive antagonism, H12 was repositioned to block AF-2, preventing binding of the coactivator. While complexed with the corepressor, hydrophobic and hydrophilic residues on H12 formed hydrophobic and hydrophilic regions, which enhanced or weakened hydrophobic interaction with the corepressor and determined the occurrence of active antagonism.

Contributions of residues to $\Delta G_{cor-rTR}$ indicated that key residues, especially hydrophobic and hydrophilic residues on H12, were essential for interactions between TR and the coactivator (Table S2). Equilibrated conformations showed that the corepressor motif (LEDIIRKALMG)[41] was stably positioned in the corepressor binding site of unbound TRα and formed an H-bond with residues K234 and K252 (Figure 5A). Every fourth residue of the corepressor (Leu1, Ile5, and Leu9) was oriented to the corepressor binding surface of TRα. The corepressor binding surface of TRα, which partly overlaps AF-2, consists of residues T223, I226, T227, V229, V230, K234, I248, K252, and C255 (for TRβ, T277, I280, T281, V283, V284, K288, I302, K306, and C309, respectively).[42] Due to hydrophobic interactions of Leu1, Ile5, and Leu9 with the hydrophobic region composed of hydrophobic residues I226, V229, V230, I248, and C255, the corepressor is able to bind to unbound TR. Interactions of 4-HO-BDE-188-bound TRα and 6-HO-BDE-90-bound TRβ with the corepressor were similar to that of unbound TRα (Figure 5 B and C). The hydrophobic residue L402 on H12 of TRα bound to 4-HO-BDE-188 formed a hydrophobic surface that interacted with hydrophobic Ile4 on the corepressor, which decreased the contribution of H12 to $\Delta G_{cor-rTR}$ (Figure 5B and Table S2). However, the hydrophobic residue on the side of the corepressor did not interact well with the hydrophilic surface generated by E449, P452, and P453 on H12 of 6-HO-BDE-90-bound TRβ, which increased the contribution of H12 to $\Delta G_{cor-rTR}$ and thus decreased the interaction between TR and the corepressor (Figure 5C and Table S2).

Mechanism Based Quantitative Prediction. Binding free energy can be an effective predictor of TH disrupting potency (see the Supporting Information). Binding free energy of HO-PBDE with TR was calculated after MD simulation of

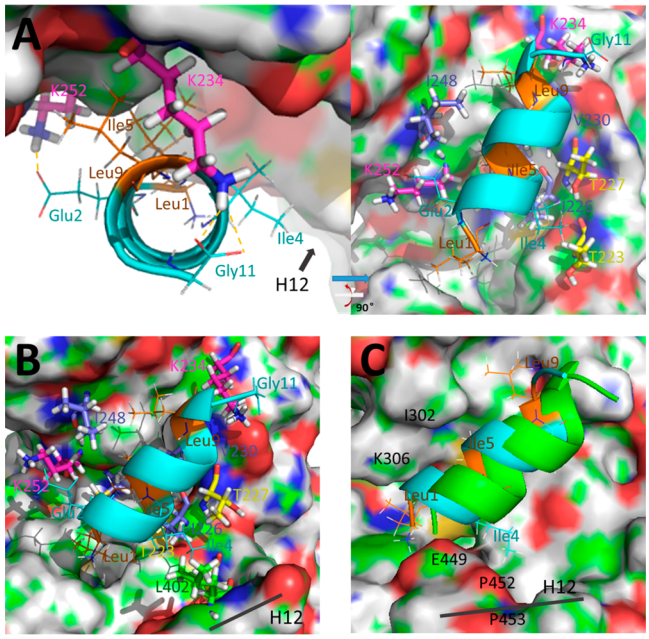

Figure 5. Close-up view of rat TRα/TRβ complexed with the corepressor peptide: (A) unbound TRα, (B) 4-HO-BDE-188-bound TRα, and (C) 6-HO-BDE-bound TRβ. Main parts of the LBDs are shown as surface. Corepressors in cyan are shown as cartoon. Residues forming H-bonds (yellow dotted lines) are colored red. Key residues are labeled. The corepressor of unbound TRα (green helix in C) is aligned to 6-HO-BDE-bound TRβ.

the HO-PBDE-TR complex ($\Delta G_{lig-rTR\alpha}$ and $\Delta G_{lig-rTR\beta}$) (Table 1). A linear relationship between combined binding free energy ($\Delta G_{sum,lig-rTR}$) and −logRIC$_{20}$ was obtained (Figure 6A), indicating that anti-TH activity of HO-PBDE was correlated with binding free energy. With coefficient of determination (R^2) of 0.754, the correlation was better than that reported previously by using binding energy obtained in molecular docking (R = 0.685)[13] and that determined by use of settling time of H12 obtained from MD simulations (R^2 = 0.6424).[26] Previous studies have focused on dissociation pathways using MD simulations to interpret the ligand-TR interactions and assess the relative TH activities, which were based on structural comformations.[47,48] Binding free energy depicts the interaction between ligand and TR in terms of free energy,[28] which is quantitative and more practical.

After interaction with the corepressor, binding free energy for HO-PBDE binding to TR ($\Delta G_{lig-rTR\alpha/cor}$, $\Delta G_{lig-rTR\beta/cor}$) changed to a different scale. 3-HO-BDE-100 strengthened the ligand-TR interaction with both TRα and TRβ; however, 2′-HO-BDE-66 weakened that interaction. Meanwhile, 2′-HO-BDE-68 strengthened the ligand-TR interaction with TRβ and weakened that with TRα. After active and passive antagonists were identified among HO-PBDEs, the combined binding free energy $\Delta G_{pas/act}$ combining binding free energies of passive and active antagonists of TRα and TRβ was calculated (eq 2) to obtain a correlation plot between $\Delta G_{pas/act}$ and −logRIC$_{20}$ (Figure 6B). With coefficient of determination (R^2 = 0.834), the correlation was greater than that of $\Delta G_{sum,lig-rTR}$. The results indicated the importance of considering effects of coregulators in MD simulations of TR. During MD simulations, which can be considered as progress of induce-fit, ligand, receptor, and corepressor fit with each other in the ligand−receptor−corepressor system.[49,50] Most previous studies with

DOI: 10.1021/acs.est.6b02029
Environ. Sci. Technol. 2016, 50, 12429−12438

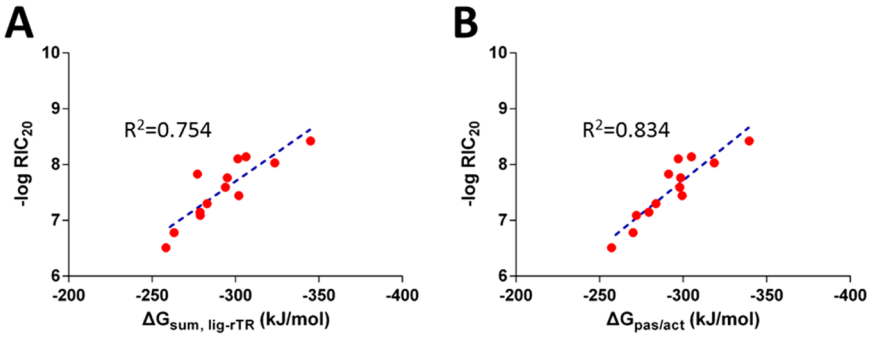

Figure 6. Correlations between anti-TH potencies and (A) sum of binding free energy of HO-PBDEs with TRα and TRβ and (B) combined binding free energy of HO-PBDEs with TRα and TRβ as passive or active antagonists.

MD simulations were carried out without consideration of coregulators which are essential for the function of the TR.[51,52] For passive TR antagonists, no coregulator was bound to the ligand−receptor complex, while for active antagonists, the corepressor was recruited to form a ligand−receptor−corepressor complex. Investigations have been carried out for better prediction by utilizing more accurate computing methods, e.g. combined quantum mechanical and molecular mechanical (QM/MM) methods, but not always obtained better prediction.[53,54] In the present investigation, after considering functioning of coregulators and the mechanism of passive and active antagonists, the determination coefficient increased from 0.754 to 0.834, revealing the importance of the coregulator and improving understanding of the mechanism by which ligands interact with TR.

In the present investigation, coregulators were introduced to investigate mechanisms of the TH disrupting effect of HO-PBDEs. Based on an understanding of coregulators, an improved method was employed to explore the interaction between HO-PBDEs, TR, and coregulators using MD simulations and protein docking. HO-PBDEs were found to exert anti-TH activities by inducing H12 to block binding of the coactivator (passive antagonist) or recruiting of the corepressor (active antagonist) for the first time. Passive and active antagonisms were further used to qualitatively identify HO-PBDEs as TR antagonists. To our knowledge, no research has been conducted to identify chemicals as TR agonists or antagonists by MD simulations. Based on the mechanism interpretation, we managed to identify HO-PBDEs as passive and active TR antagonists according to the role of coregulators. Finally, ligand−receptor binding free energy was used to quantitatively predict the anti-TH activities of HO-PBDEs. Binding free energy considering mechanisms of passive and active antagonisms ($\Delta G_{pas/act}$) obtained better prediction than $\Delta G_{sum,lig-rTR}$ and was regarded as a predictor of anti-TH activity.

It is clear from the results presented here and a growing list of other examples that assessing whether a contaminant is likely to be a disruptor of hormone function based solely on its ability to bind to the LBD of the respective receptor is far too simplistic. Thus, this approach is worthy of application to other endocrine disrupting chemicals. It is recommended that endocrine disrupting chemicals be qualitatively identified and the disrupting potencies be quantitatively predicted following the protocol (Figure 1). However, it should be considered whether or not the compounds are able to bind to the receptor before performing simulations, which is the foundation of the following simulations. QSAR and structural similarity calculation will be beneficial because structurally similar compounds always bind to similar target receptors.[55]

■ ASSOCIATED CONTENT

Supporting Information

The Supporting Information is available free of charge on the ACS Publications website at DOI: 10.1021/acs.est.6b02029.

Supporting materials and additional information for this text, including Tables S1 and S2 and Figures S1−S6 (PDF)

■ AUTHOR INFORMATION

Corresponding Authors

*E-mail: njushiwei@nju.edu.cn (W.S).
*E-mail: yuhx@nju.edu.cn (H.Y.).

Notes

The authors declare no competing financial interest.

■ ACKNOWLEDGMENTS

This work was supported by the Natural Science Foundation of China (21577058 and 21307054), Nonprofit industry research subject (201409040), the Natural Science Foundation of Jiangsu Province (BK20130551), the Major Science and Technology Program for Water Pollution Control and Treatment (2012ZX07101-003), the Specialized Research Fund for the Doctoral Program of Higher Education (20130091120013), and the Collaborative Innovation Center for Regional Environmental Quality. The computational calculations were performed on the IBM Blade cluster system in the High Performance Computing Center (HPCC) of Nanjing University. The HO-PBDEs were kindly provided by Michael H. W. Lam (Department of Biology and Chemistry, City University of Hong Kong). Prof. Giesy was supported by the program of 2012 "High Level Foreign Experts" (#GDT20143200016) funded by the State Administration of Foreign Experts Affairs, the P.R. China to Nanjing University, and the Einstein Professor Program of the Chinese Academy of Sciences. He was also supported by the Canada Research Chair program and a Distinguished Visiting Professorship in the School of Biological Sciences of the University of Hong Kong.

■ REFERENCES

(1) Wan, Y.; Wiseman, S.; Chang, H.; Zhang, X.; Jones, P. D.; Hecker, M.; Kannan, K.; Tanabe, S.; Hu, J.; Lam, M. H.; Giesy, J. P. Origin of hydroxylated brominated diphenyl ethers: natural compounds or man-made flame retardants? *Environ. Sci. Technol.* **2009**, *43* (19), 7536−7542.

DOI: 10.1021/acs.est.6b02029
Environ. Sci. Technol. 2016, 50, 12429−12438

(2) Wiseman, S. B.; Wan, Y.; Chang, H.; Zhang, X.; Hecker, M.; Jones, P. D.; Giesy, J. P. Polybrominated diphenyl ethers and their hydroxylated/methoxylated analogs: environmental sources, metabolic relationships, and relative toxicities. *Mar. Pollut. Bull.* **2011**, *63* (5), 179−188.
(3) Wang, S.; Zhang, S.; Huang, H.; Niu, Z.; Han, W. Characterization of polybrominated diphenyl ethers (PBDEs) and hydroxylated and methoxylated PBDEs in soils and plants from an e-waste area, China. *Environ. Pollut.* **2014**, *184*, 405−413.
(4) Yu, B.; Zhang, R.; Liu, P.; Zhang, Y.; Zhang, Y.; Bai, Y. Determination of nine hydroxylated polybrominated diphenyl ethers in water by precolumn derivatization-gas chromatography−mass spectrometry. *J. Chromatogr. A* **2015**, *1419*, 19−25.
(5) Kim, U.; Jo, H.; Lee, I.; Joo, G.; Oh, J. Investigation of bioaccumulation and biotransformation of polybrominated diphenyl ethers, hydroxylated and methoxylated derivatives in varying trophic level freshwater fishes. *Chemosphere* **2015**, *137*, 108−114.
(6) Wang, H.; Chen, Z.; Ho, K.; Ge, L.; Du, J.; Lam, M. H.; Giesy, J. P.; Wong, M.; Wong, C. K. Hydroxylated and methoxylated polybrominated diphenyl ethers in blood plasma of humans in Hong Kong. *Environ. Int.* **2012**, *47*, 66−72.
(7) Chen, A.; Park, J. S.; Linderholm, L.; Rhee, A.; Petreas, M.; DeFranco, E. A.; Dietrich, K. N.; Ho, S. Hydroxylated polybrominated diphenyl ethers in paired maternal and cord sera. *Environ. Sci. Technol.* **2013**, *47* (8), 3902−3908.
(8) Kitamura, S.; Shinohara, S.; Iwase, E.; Sugihara, K.; Uramaru, N.; Shigematsu, H.; Fujimoto, N.; Ohta, S. Affinity for thyroid hormone and estrogen receptors of hydroxylated polybrominated diphenyl ethers. *J. Health Sci.* **2008**, *54* (5), 607−614.
(9) Ren, X.; Guo, L.; Gao, Y.; Zhang, B.; Wan, B. Hydroxylated polybrominated diphenyl ethers exhibit different activities on thyroid hormone receptors depending on their degree of bromination. *Toxicol. Appl. Pharmacol.* **2013**, *268* (3), 256−263.
(10) Liu, H.; Hu, W.; Sun, H.; Shen, O.; Wang, X.; Lam, M. H.; Giesy, J. P.; Zhang, X.; Yu, H. In vitro profiling of endocrine disrupting potency of 2, 2′, 4, 4′-tetrabromodiphenyl ether (BDE47) and related hydroxylated analogs (HO-PBDEs). *Mar. Pollut. Bull.* **2011**, *63* (5), 287−296.
(11) Meerts, I.; Letcher, R. J.; Hoving, S.; Marsh, G.; Bergman, A.; Lemmen, J. G.; van der Burg, B.; Brouwer, A. In vitro estrogenicity of polybrominated diphenyl ethers, hydroxylated PDBEs, and polybrominated bisphenol A compounds. *Environ. Health. Persp.* **2001**, *109* (4), 399.
(12) Nakamura, N.; Matsubara, K.; Sanoh, S.; Ohta, S.; Uramaru, N.; Kitamura, S.; Yamaguchi, M.; Sugihara, K.; Fujimoto, N. Cell type-dependent agonist/antagonist activities of polybrominated diphenyl ethers. *Toxicol. Lett.* **2013**, *223* (2), 192−197.
(13) Li, F.; Xie, Q.; Li, X.; Li, N.; Chi, P.; Chen, J.; Wang, Z.; Hao, C. Hormone activity of hydroxylated polybrominated diphenyl ethers on human thyroid receptor-β: in vitro and in silico investigations. *Environ. Health. Persp.* **2010**, *118* (5), 602−606.
(14) Yu, H.; Wondrousch, D.; Li, F.; Chen, J.; Lin, H.; Ji, L. In Silico Investigation of the Thyroid Hormone activity of hydroxylated polybrominated diphenyl ethers. *Chem. Res. Toxicol.* **2015**, *28* (8), 1538−1545.
(15) Clark, R. D.; Norinder, U. Two personal perspectives on a key issue in contemporary 3D QSAR. *WIREs. Comput. Mol. Sci.* **2012**, *2* (1), 108−113.
(16) Mangoni, M.; Roccatano, D.; Di Nola, A. Docking of flexible ligands to flexible receptors in solution by molecular dynamics simulation. *Proteins: Struct., Funct., Genet.* **1999**, *35* (2), 153−162.
(17) Martínez, L.; Webb, P.; Polikarpov, I.; Skaf, M. S. Molecular dynamics simulations of ligand dissociation from thyroid hormone receptors: evidence of the likeliest escape pathway and its implications for the design of novel ligands. *J. Med. Chem.* **2006**, *49* (1), 23−26.
(18) Barettino, D.; Ruiz, M. V.; Stunnenberg, H. Characterization of the ligand-dependent transactivation domain of thyroid hormone receptor. *EMBO. J.* **1994**, *13* (13), 3039.
(19) Shibata, H.; Spencer, T. E.; Oñate, S. A.; Jenster, G.; Tsai, S. Y.; Tsai, M.; O'Malley, B. W. Role of co-activators and co-repressors in the mechanism of steroid/thyroid receptor action. *Recent. Prog. Horm. Res.* **1996**, *52*, 141−164.
(20) Glass, C. K.; Rose, D. W.; Rosenfeld, M. G. Nuclear receptor coactivators. *Curr. Opin. Cell Biol.* **1997**, *9* (2), 222−232.
(21) Estebanez-Perpina, E.; Arnold, L. A.; Jouravel, N.; Togashi, M.; Blethrow, J.; Mar, E.; Nguyen, P.; Phillips, K. J.; Baxter, J. D.; Webb, P. Structural insight into the mode of action of a direct inhibitor of coregulator binding to the thyroid hormone receptor. *Mol. Endocrinol.* **2007**, *21* (12), 2919−2928.
(22) Wen, L.; Shi, Y. Unliganded thyroid hormone receptor α controls developmental timing in Xenopus tropicalis. *Endocrinology* **2015**, *156* (2), 721−734.
(23) Baniahmad, A.; Leng, X.; Burris, T. P.; Tsai, S. Y.; Tsai, M.; O'Malley, B. W. The tau 4 activation domain of the thyroid hormone receptor is required for release of a putative corepressor (s) necessary for transcriptional silencing. *Mol. Cell. Biol.* **1995**, *15* (1), 76−86.
(24) Arnold, L. A.; Estébanez-Perpiñá, E.; Togashi, M.; Jouravel, N.; Shelat, A.; McReynolds, A. C.; Mar, E.; Nguyen, P.; Baxter, J. D.; Fletterick, R. J. Discovery of small molecule inhibitors of the interaction of the thyroid hormone receptor with transcriptional coregulators. *J. Biol. Chem.* **2005**, *280* (52), 43048−43055.
(25) Schoch, G. A.; D'Arcy, B.; Stihle, M.; Burger, D.; Bär, D.; Benz, J.; Thoma, R.; Ruf, A. Molecular switch in the glucocorticoid receptor: active and passive antagonist conformations. *J. Mol. Biol.* **2010**, *395* (3), 568−577.
(26) Wang, X.; Yang, H.; Hu, X.; Zhang, X.; Zhang, Q.; Jiang, H.; Shi, W.; Yu, H. Effects of HO-/MeO-PBDEs on androgen receptor: in vitro investigation and helix 12-involved MD simulation. *Environ. Sci. Technol.* **2013**, *47* (20), 11802−11809.
(27) Honig, B.; Yang, A. Free energy balance in protein folding. *Adv. Protein. Chem.* **1995**, *46*, 27−58.
(28) Kumari, R.; Kumar, R.; Lynn, A. g_mmpbsa: a GROMACS tool for high-throughput MM-PBSA calculations. *J. Chem. Inf. Model.* **2014**, *54* (7), 1951−1962.
(29) Brown, S. P.; Muchmore, S. W. High-throughput calculation of protein-ligand binding affinities: modification and adaptation of the MM-PBSA protocol to enterprise grid computing. *J. Chem. Inf. Model.* **2006**, *46* (3), 999−1005.
(30) Yang, Y.; Qin, J.; Liu, H.; Yao, X. Molecular dynamics simulation, free energy calculation and structure-based 3D-QSAR studies of B-RAF kinase inhibitors. *J. Chem. Inf. Model.* **2011**, *51* (3), 680−692.
(31) Harris, J. B.; Eldridge, M. L.; Sayler, G.; Menn, F. M.; Layton, A. C.; Baudry, J. A computational approach predicting CYP450 metabolism and estrogenic activity of an endocrine disrupting compound (PCB-30). *Environ. Toxicol. Chem.* **2014**, *33* (7), 1615−1623.
(32) Marsh, G.; Stenutz, R.; Bergman, A. Synthesis of hydroxylated and methoxylated polybrominated diphenyl ethers− natural products and potential polybrominated diphenyl ether metabolites. *Eur. J. Org. Chem.* **2003**, *2003* (14), 2566−2576.
(33) Ghisari, M.; Bonefeld-Jorgensen, E. C. Impact of environmental chemicals on the thyroid hormone function in pituitary rat GH3 cells. *Mol. Cell. Endocrinol.* **2005**, *244* (1), 31−41.
(34) Yang, W.; Shen, S.; Mu, L.; Yu, H. Structure−activity relationship study on the binding of PBDEs with thyroxine transport proteins. *Environ. Toxicol. Chem.* **2011**, *30* (11), 2431−2439.
(35) Hess, B.; Kutzner, C.; Van Der Spoel, D.; Lindahl, E. GROMACS 4: algorithms for highly efficient, load-balanced, and scalable molecular simulation. *J. Chem. Theory Comput.* **2008**, *4* (3), 435−447.
(36) Berendsen, H. J.; van der Spoel, D.; van Drunen, R. GROMACS: A message-passing parallel molecular dynamics implementation. *Comput. Phys. Commun.* **1995**, *91* (1), 43−56.
(37) Baker, N. A.; Sept, D.; Joseph, S.; Holst, M. J.; McCammon, J. A. Electrostatics of nanosystems: application to microtubules and the ribosome. *Proc. Natl. Acad. Sci. U. S. A.* **2001**, *98* (18), 10037−10041.

DOI: 10.1021/acs.est.6b02029
Environ. Sci. Technol. 2016, 50, 12429−12438

(38) Ozers, M. S.; Ervin, K. M.; Steffen, C. L.; Fronczak, J. A.; Lebakken, C. S.; Carnahan, K. A.; Lowery, R. G.; Burke, T. J. Analysis of ligand-dependent recruitment of coactivator peptides to estrogen receptor using fluorescence polarization. *Mol. Endocrinol.* **2005**, *19* (1), 25−34.
(39) Ren, X.; Guo, L. Assessment of the Binding of Hydroxylated Polybrominated Diphenyl Ethers to Thyroid Hormone Transport Proteins Using a Site-Specific Fluorescence Probe. *Environ. Sci. Technol.* **2012**, *46* (8), 4633−4640.
(40) Su, G.; Yu, H.; Lam, M. H.; Giesy, J. P.; Zhang, X. Mechanisms of toxicity of hydroxylated polybrominated diphenyl ethers (HO-PBDEs) determined by toxicogenomic analysis with a live cell array coupled with mutagenesis in Escherichia coli. *Environ. Sci. Technol.* **2014**, *48* (10), 5929−5937.
(41) Kojima, H.; Takeuchi, S.; Uramaru, N.; Sugihara, K.; Yoshida, T.; Kitamura, S. Nuclear hormone receptor activity of polybrominated diphenyl ethers and their hydroxylated and methoxylated metabolites in transactivation assays using Chinese hamster ovary cells. *Environ. Health. Persp.* **2009**, *117* (8), 1210−1218.
(42) Moriyama, K.; Tagami, T.; Akamizu, T.; Usui, T.; Saijo, M.; Kanamoto, N.; Hataya, Y.; Shimatsu, A.; Kuzuya, H.; Nakao, K. Thyroid hormone action is disrupted by bisphenol A as an antagonist. *J. Clin. Endocrinol. Metab.* **2002**, *87* (11), 5185−5190.
(43) Li, L.; Andersen, M. E.; Heber, S.; Zhang, Q. Non-monotonic dose−response relationship in steroid hormone receptor-mediated gene expression. *J. Mol. Endocrinol.* **2007**, *38* (5), 569−585.
(44) Glass, C. K.; Rosenfeld, M. G. The coregulator exchange in transcriptional functions of nuclear receptors. *Gene. Dev.* **2000**, *14* (2), 121−141.
(45) Kawai, K.; Sasaki, S.; Morita, H.; Ito, T.; Suzuki, S.; Misawa, H.; Nakamura, H. Unliganded thyroid hormone receptor-β1 represses liver X receptor α/oxysterol-dependent transactivation. *Endocrinology* **2004**, *145* (12), 5515−5524.
(46) Souza, P. C.; Barra, G. B.; Velasco, L. F.; Ribeiro, I. C.; Simeoni, L. A.; Togashi, M.; Webb, P.; Neves, F. A.; Skaf, M. S.; Martinez, L. Helix 12 dynamics and thyroid hormone receptor activity: experimental and molecular dynamics studies of Ile280 mutants. *J. Mol. Biol.* **2011**, *412* (5), 882−893.
(47) Martínez, L.; Sonoda, M. T.; Webb, P.; Baxter, J. D.; Skaf, M. S.; Polikarpov, I. Molecular dynamics simulations reveal multiple pathways of ligand dissociation from thyroid hormone receptors. *Biophys. J.* **2005**, *89* (3), 2011−2023.
(48) Martinez, L.; Polikarpov, I.; Skaf, M. S. Only subtle protein conformational adaptations are required for ligand binding to thyroid hormone receptors: simulations using a novel multipoint steered molecular dynamics approach. *J. Phys. Chem. B* **2008**, *112* (34), 10741−10751.
(49) Koshland, D. E. The key-lock theory and the induced fit theory. *Angew. Chem., Int. Ed. Engl.* **1995**, *33* (23−24), 2375−2378.
(50) Changeux, J.; Edelstein, S. Conformational selection or induced fit? 50 years of debate resolved. *F1000 Biol. Rep.* **2011**, *3*, 19.
(51) Martínez, J. M.; Martínez, L. Packing optimization for automated generation of complex system's initial configurations for molecular dynamics and docking. *J. Comput. Chem.* **2003**, *24* (7), 819−825.
(52) Gupta, M. K.; Misra, K. Atom-based 3D-QSAR, molecular docking and molecular dynamics simulation assessment of inhibitors for thyroid hormone receptor α and β. *J. Mol. Model.* **2014**, *20* (6), 1−19.
(53) Freindorf, M.; Furlani, T. R.; Kong, J.; Cody, V.; Davis, F. B.; Davis, P. J. Combined QM/MM Study of Thyroid and Steroid Hormone Analogue Interactions with $\alpha v\beta 3$ Integrin. *J. Biomed. Biotechnol.* **2012**, *2012*, 1−12.
(54) Slynko, I.; Scharfe, M.; Rumpf, T.; Eib, J.; Metzger, E.; Schüle, R.; Jung, M.; Sippl, W. Virtual screening of PRK1 inhibitors: ensemble docking, rescoring using binding free energy calculation and QSAR model development. *J. Chem. Inf. Model.* **2014**, *54* (1), 138−150.
(55) Schuffenhauer, A.; Floersheim, P.; Acklin, P.; Jacoby, E. Similarity metrics for ligands reflecting the similarity of the target proteins. *J. Chem. Inf. Model.* **2003**, *43* (2), 391−405.

DOI: 10.1021/acs.est.6b02029
Environ. Sci. Technol. 2016, 50, 12429−12438

Supporting Information for

Identification of thyroid hormone disruptors among HO-PBDEs: *In vitro* investigation and co-regulator involved simulation

Qinchang Chen[†], Xiaoxiang Wang[†, ‡], Wei Shi[†, *], Hongxia Yu[†, *], Xiaowei Zhang[†], John P. Giesy[†, §, ∥, ⊥]

[†] State Key Laboratory of Pollution Control and Resources Reuse, School of the Environment, Nanjing University, Nanjing, PR China

[‡] Multiphase Chemistry Department, Max Planck Institute for Chemistry, 55128 Mainz, Germany

[§] Department of Veterinary Biomedical Sciences and Toxicology Centre, University of Saskatchewan, Saskatoon, Saskatchewan, Canada.

[∥] Department of Zoology, and Center for Integrative Toxicology, Michigan State University, East Lansing, MI, USA

[⊥] School of Biological Sciences, University of Hong Kong, Hong Kong, SAR, China

[*]Corresponding author: Wei Shi: njushiwei@nju.edu.cn; Hongxia Yu: yuhx@nju.edu.cn

This file includes:

Pages: S1-S22

Tables: S1-S2

Figures: S1-S6

Synthesis of Fluorescein-labeled T3 (F-T_3)

F-T_3 probe was prepared for use in the competitive binding assay, by use of a previously described method.[1] Crude products were incubated from reaction of fluorescein isothiocyanate (Sigma, St. Louis, MO, USA) and T_3 in a medium of pyridine/water/triethylamine (9:1.5:0.1, v/v/v) mixture for 1 hour at 37 °C, and precipitated with 20 volumes of ammonium acetate buffer (0.2 M, pH 4.0). Products were washed by distilled water after centrifugation (10 min, 1000g). Centrifuged precipitate was then redissolved in 0.05 M NH4HCO3 and purified by a small Sephadex G-75 column (0.9 × 10 cm). Equilibration and elution were carried out with 0.05 M NH4HCO3 and distilled water, respectively. Synthetic F-T_3 was freeze-dried and determined to have a correct molecular weight of 1049.8 by Matrix-Assisted Laser Desorption Ionization-Time of Flight Mass Spectrometry (MALDI-TOF MS; ABSciex, Foster City, CA, USA). The concentration of stock solution in Tris−NaCl buffer (50 mM Tris−HCl/100 mM NaCl, pH 7.4) was determined by its absorbance at 490 nm with a reported molar extinction coefficient of $7.8 \times 10^4\ M^{-1}\ cm^{-1}$.

Competitive binding assay

A mixture of 45 nM fluorescent probe F-T_3, 180 nM TR-LBDs and various concentrations of HO-PBDEs or T_3 in assay buffer (150 mM KCl, 50 mM potassium phosphate, 0.5 mM EDTA, pH 8.0) with total volume of 20 μL was added to each well of a black 384-well plate (Nunc). After 5-min incubation at room temperature, fluorescence polarization was measured on a Synergy H4 microplate reader (BioTek, Winooski, VT, USA) with a 485/20-excitation filter and a 528/20-emission filter. The reader was controlled and polarization values automatically computed

by use of Gen5 (BioTek).

Coactivator recruitment assay

A 20 μL mixture of 45 nM peptide, 180 nM TR-LBDs and various concentrations of HO-PBDEs or T_3 in buffer C (Life Technology) was added to every well of a black 384 well plate (Corning, Corning, NY, USA). Incubation and polarization detection were the same as the competitive binding assay.

GH3 cell proliferation assay

The rat pituitary cell line GH3 was cultured as recommended by China Infrastructure of Cell Line Resources (Beijing, China). The cell line was maintained in Ham's F10 Nutrient Mixture (from China Infrastructure of Cell Line Resources) supplemented with 2.5% fetal bovine serum (FBS, Gibco, Invitrogen Corporation, Carlsbad, CA, USA) and 15% Donor Equine Serum (DES, HyClone, Logan, UT, USA) at 37 ˚C in a humidified atmosphere of 5% CO2. Serum-free medium was used instead of the standard culture medium 48 hours before the cells were seeded to 96 well plate (Corning, Corning, NY, USA). The serum-free medium is a mixture of Ham's F10 Nutrient Mixture with 10 μM ethanolamine, 10 μg/mL bovine insulin, 10 μg/mL human apotransferrin, 500 μg/mL bovine serum albumin and 10 ng/mL sodium selenite.[1] Penicillin (100 units/mL) was added to inhibit bacterial growth. Then GH3 cells were seeded into 96-well plates in a density of 2500 cells per well. Ligands were diluted to different concentrations in the serum-free medium with or without the addition of T_3 and added to the wells with a total volume of 100 μL. CellTiter 96® AQueous One Solution Cell Proliferation Assay Kit (Promega, Madison, WI, USA) was used to assess the proliferation of the GH3 cells. After 4-day's incubation, 20 μL of

the CellTiter 96® AQueous One Solution Reagent was pipetted into each well and incubated for 3 hours. Finally, absorbance at 490 nm was recorded using a Synergy H4 microplate reader (BioTek, Winooski, VT, USA).

Structure preparation and docking

Initial compounds of the tested ligands were built according to the structurally analogous compounds from NCBI PubChem Compound (http://www.ncbi.nlm.nih.gov/pccompound). Structural energy minimization was carried out to optimize the geometries of these compounds using Powell gradient algorithm and the Tripos force field[2] by the Minimize module in SYBYL7.3 (Tripos Inc., St. Louis, MO, USA). Homology modeling of apo thyroid hormone receptor ligand binding domains (TR-LBDs) were done using Swiss-Model[3-6] online modeling system (http://swissmodel.expasy.org/), automated mode. Crystal structures of human TRα (PDB code: 4LNX) and TRβ (PDB code: 1NQ0) were chosen from RCSB Protein Data Bank (http://www.rcsb.org/pdb/home/home.do) and used as templates for homology modeling of both human and rat TR-LBDs. To build the apo conformation, structure of apo ER-LBD (PDB code: 1A52) was used as a template to build H11-H12 loop of each LBD. Quality of the built TR-LBDs were evaluated with Ramachandran plot[7,8] (Figure S2) generated by the Structure Analysis and Verification Server (SAVES, http://services.mbi.ucla.edu/SAVES/). Then the Surflex-Dock[9] program interfaced with SYBYL 7.3 was used to dock the optimized ligands into the docking cavities of TR-LBDs. Details of the docking process has been previously described. Complexes of receptors and ligands were generated for MD simulations.

Molecular dynamics simulations

CHARMM 27 force field[10, 11] was employed to the structures, using the GROMACS 4.5 package[12, 13] for TRs and SwissParam[14] (http://www.swissparam.ch/) for ligands. The system was immersed with TIP3P water molecules[15] in a box, keeping the minimum distance between the complex and the boundary larger than 1.4 nm. Na+ and Cl- ions were added to neutralize the system. All MD simulations were performed in the NPT ensemble with periodic boundary conditions using GROMACS 4.5 package on an International Business Machines (IBM) Blade cluster system. Electrostatic interactions were calculated with the particle mesh Ewald method, with van der Waals interactions cutoff of 1.0 nm. Simulations were performed for at least 15 ns using a 2 fs time step, and snapshots for analysis were saved every 2 ps.

Docking of co-regulators using Hex 8.0.0

Corepressor motifs (PDB code: 2OVM) and coactivator motifs (PDB code: 2B1V) were pre-positioned on the co-regulator binding surface according to the previous publications.[16-18] The protein docking program, Hex 8.0.0,[19] was used to modify the positions of co-regulators and give a shape-based docking score E_{dock}. Co-regulators were then docked to the extracted TRs using shape-based 3D fast Fourier transform (FFT) docking methods. The receptor and ligand range angles were all set to 15 degrees to make sure the co-regulators did not rotate far away from the reference positions.

Calculation of MM-PBSA binding free energy

Trajectories obtained from MD simulations were used for binding free energy calculations

using molecular mechanics Poisson-Boltzmann surface area (MM-PBSA) method. Generally, binding free energy $\Delta G_{binding}$ can be defined (Equation S1).

$$\Delta G_{binding} = G_{complex} - (G_{receptor} + G_{ligand}) \quad (S1)$$

where $G_{complex}$, $G_{receptor}$ and G_{ligand} are total free energies of the receptor-ligand complex, receptor, and ligand in solvent, respectively. The G value for each term (G_x) can be calculated (Equation S2).

$$G_x = E_{MM} - TS + G_{solvation} \quad (S2)$$

where E_{MM} is the molecular mechanics energy; TS denotes the entropic contribution where T and S refer to the temperature and entropy, respectively; $G_{solvation}$ is the solvation free energy.

Molecular mechanics energy E_{MM} includes the energy of bonded (E_{bonded}), electrostatic ($E_{electrostatic}$) and van der Waals (E_{vdW}) interactions (Equation S3).

$$E_{MM} = E_{bonded} + E_{electrostatic} + E_{vdW} \quad (S3)$$

Solvation free energy $G_{solvation}$ can be divided into two parts, electrostatic (G_{polar}) and nonelectrostatic ($G_{nonpolar}$) solvation free energy (Equation S4).

$$G_{solvation} = G_{polar} + G_{nonpolar} \quad (S4)$$

$G_{nonpolar}$ was calculated based on the solvent accessible surface area (SASA) model.

Snapshots extracted from MD trajectories at intervals of 100 ps were used for calculation of MM-PBSA binding free energy. All calculations of MM-PBSA were performed by use of the g_mmpbsa package[20] developed form GROMACS and APBS[21] programs.

Conformational dynamics and equilibrated conformations

During the MD simulations, the ligand-receptor complexes experienced conformational dynamics

and pose of TR, especially H12 significantly changed. RMSD of H12 of every ligand-bound human TRα/TRβ-LBD (ligand-hTRα/TRβ-H12) was calculated to assess the reposition of H12. The RMSD of T_3-hTRα-H12 became stable at about 6 ns (Figure S4A), indicating a stable reposition of H12 in 6 ns. Similarly, 2-HO-BDE-123-hTRα-H12, 3-HO-BDE-100-hTRβ-H12 and most of the H12s of HO-PBDE-bound TRα and TRβ became stable within 15 ns (Figure S4). Similar results were observed in rat TRα/TRβ-LBD (Figure S5). However, some HO-PBDEs didn't equilibrate TRα or TRβ even when the simulation was prolonged to 22 ns (Figure S5 C and F). Dynamic trajectories of LBDs occupied by different HO-PBDEs which couldn't equilibrate H12 in 20 ns were observed to find H12s moving irregularly in certain regions (data not shown), and the fluctuation range tended to reduce. Therefore, representative snapshots of the equilibrating trajectories were extracted and considered as equilibrated conformations.

147 **Table S1. Binding free energies, docking scores and binding affinities of human TR**

Chemical	TRα			TRβ		
	ΔG (kJ/mol)	Docking Score	IC_{50}	ΔG (kJ/mol)	Docking Score	IC_{50}
T3	-167.7	6.46	3.25E-07	-169.0	6.26	2.48E-07
6-HO-BDE-137	-151.4	3.14	1.46E-04	-156.5	2.91	2.77E-05
3-HO-BDE-100	-134.9	2.25	1.38E-04	-150.5	1.52	2.32E-06
2-HO-BDE-123	-134.1	2.71	1.87E-04	-	-	-

148 **Table S2. Contributions of key residues to the binding free energy of rat TR with corepressor (kJ/mol)**

Residues	2-HO-BDE-123	2'-HO-BDE-66	2'-HO-BDE-68	3-HO-BDE-100	4'-HO-BDE-101	4'-HO-BDE-17	4-HO-BDE-188	4'-HO-BDE-49	4-HO-BDE-90
rTRα									
THR-223	-0.62	-1.80	-0.46	-1.29	-0.35	0.15	-2.29	-0.04	-2.57
ILE-226	-7.38	-4.42	-1.90	-6.76	-8.26	-7.18	-7.97	-2.76	-5.79
THR-227	0.26	-0.18	-0.20	0.18	0.12	-0.01	-2.73	-1.04	-1.90
VAL-229	0.12	-0.03	0.11	-0.08	-0.13	-0.06	-0.17	-0.26	0.78
VAL-230	-9.06	-9.03	-7.09	-9.75	-9.53	-9.78	-9.82	-8.73	-9.11
ILE-248	-13.93	-14.70	-15.35	-17.28	-14.67	-16.44	-14.19	-15.88	-16.89
CYS-255	-2.74	-1.77	-0.20	-2.41	-2.79	-2.27	-3.41	-1.65	-0.76
Key Residues	-33.35	-31.92	-25.09	-37.38	-35.60	-35.58	-40.58	-30.36	-36.24
Corepressor	-41.58	-23.57	-34.38	-43.78	-65.94	-47.25	-74.79	-33.09	-35.68
H12	-17.24	-0.22	-8.54	-8.59	-21.27	-39.09	-32.20	-6.51	-2.13

rTRβ									
THR-277	-	-1.24	-0.37	-0.57	-0.13	-0.02	-0.59	-0.11	-
ILE-280	-	-6.17	-5.79	-7.21	-0.19	-0.55	-6.67	-0.47	-
THR-281	-	-2.22	-1.07	1.32	-0.45	-0.40	0.66	-0.93	-
VAL-283	-	-0.22	-0.33	-0.33	0.21	0.28	-0.42	0.30	-
VAL-284	-	-9.69	-9.29	-10.14	-5.11	-6.98	-10.14	-6.38	-
ILE-302	-	-14.07	-15.47	-14.34	-13.54	-12.76	-17.09	-15.90	-
CYS-309	-	-2.59	-2.48	-2.61	-0.44	0.22	-2.26	0.25	-
Key Residues	-	-36.21	-34.80	-33.88	-19.65	-20.21	-36.51	-23.24	-
Corepressor	-	-20.10	-42.12	-54.20	-38.69	-49.43	-51.85	-51.22	-
H12	-	-10.81	3.05	-25.09	-10.98	-19.07	-24.15	-28.07	-

149

150

Residues	6-HO-BDE-137	6-HO-BDE-157	6'-HO-BDE-17	6-HO-BDE-47	6-HO-BDE-85	6-HO-BDE-90	6'-HO-BDE-99	Unbound
rTRα								
THR-223	-0.79	-0.05	-0.87	-0.61	-	0.16	-1.32	-0.70
ILE-226	-8.09	-1.75	-5.24	-7.37	-	-7.45	-5.97	-5.15
THR-227	-1.42	-0.10	0.48	0.82	-	1.36	-1.82	0.56
VAL-229	0.02	-0.09	-0.40	-0.24	-	-0.45	-0.24	-0.46
VAL-230	-9.33	-8.21	-9.84	-10.17	-	-10.29	-9.39	-9.47
ILE-248	-17.96	-14.68	-14.33	-16.03	-	-14.22	-16.12	-16.44
CYS-255	-2.67	-0.62	-2.49	-2.55	-	-2.86	-2.59	-2.30
Key Residues	-40.24	-25.51	-32.69	-36.15	-	-33.75	-37.47	-33.97
Corepressor	-58.04	-6.19	-43.12	-44.71	-	-46.20	-51.61	-47.83
H12	-12.53	-6.91	-12.92	-8.85	-	-9.60	-32.28	-6.58
rTRβ								

THR-277	-	-2.22	-0.17	-1.02	-0.01	-1.38	-0.11	-0.80
ILE-280	-	-7.65	-5.19	-3.54	-0.40	-5.65	-0.43	-5.76
THR-281	-	-0.25	-2.63	-3.13	-0.47	0.68	-0.96	-2.15
VAL-283	-	0.55	0.08	-0.21	0.31	0.01	0.32	-0.20
VAL-284	-	-9.01	-9.28	-9.53	-5.69	-9.05	-5.91	-9.89
ILE-302	-	-15.12	-14.02	-15.15	-13.72	-17.11	-14.32	-13.79
CYS-309	-	-1.78	-1.87	-3.13	-0.19	-2.04	0.22	-2.16
Key Residues	-	-35.48	-33.09	-35.70	-20.16	-34.55	-21.19	-34.76
Corepressor	-	-51.67	-1.93	-44.10	-79.17	12.04	-45.39	-32.09
H12	-	0.93	4.90	-20.81	-7.23	16.79	-27.06	-10.93

151

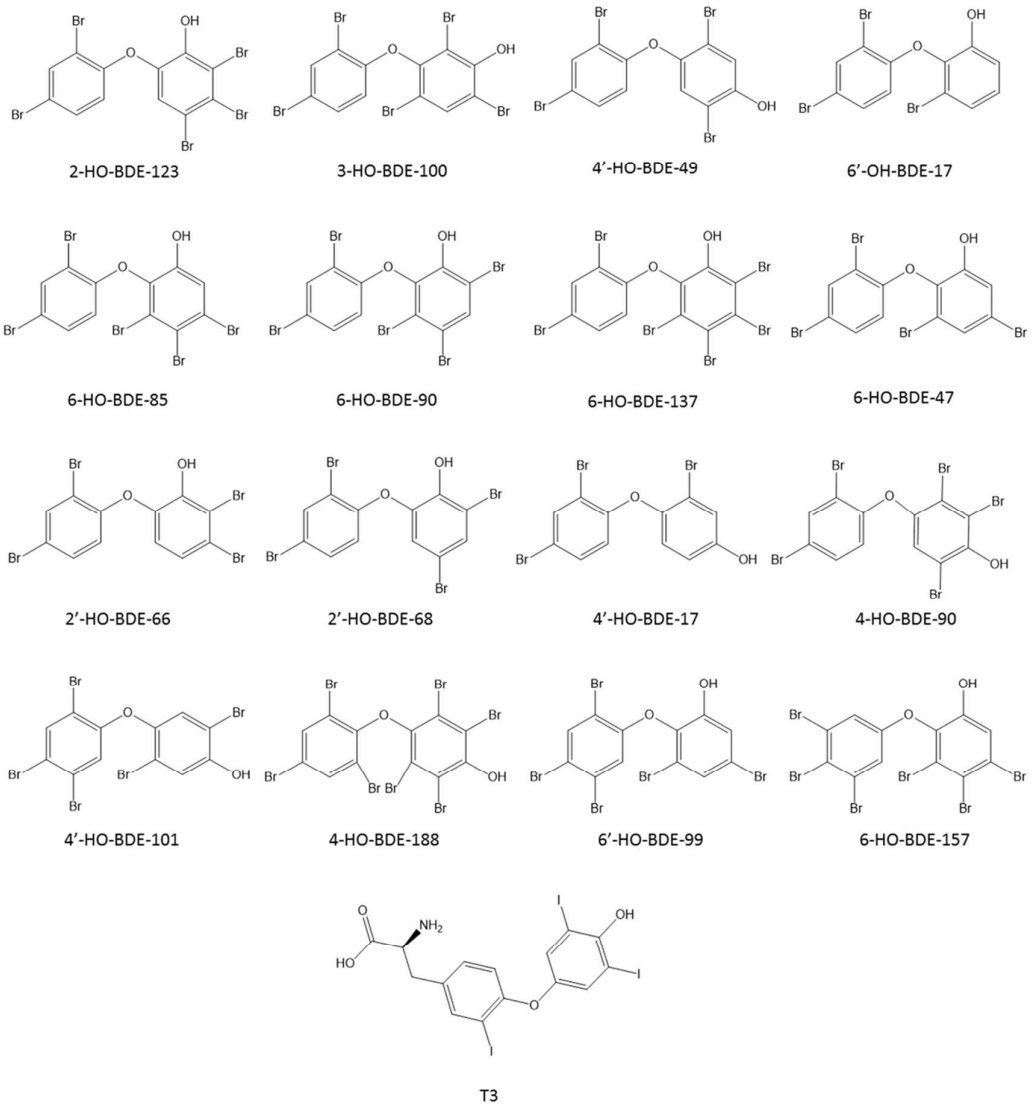

Figure S1. Molecular structures of 16 HO-PBDEs and T_3 used in the current study. HO-PBDEs in the fourth line were from AccuStandard (New Haven, CT, USA), others were from Department of Biology and Chemistry of City University of Hong Kong.

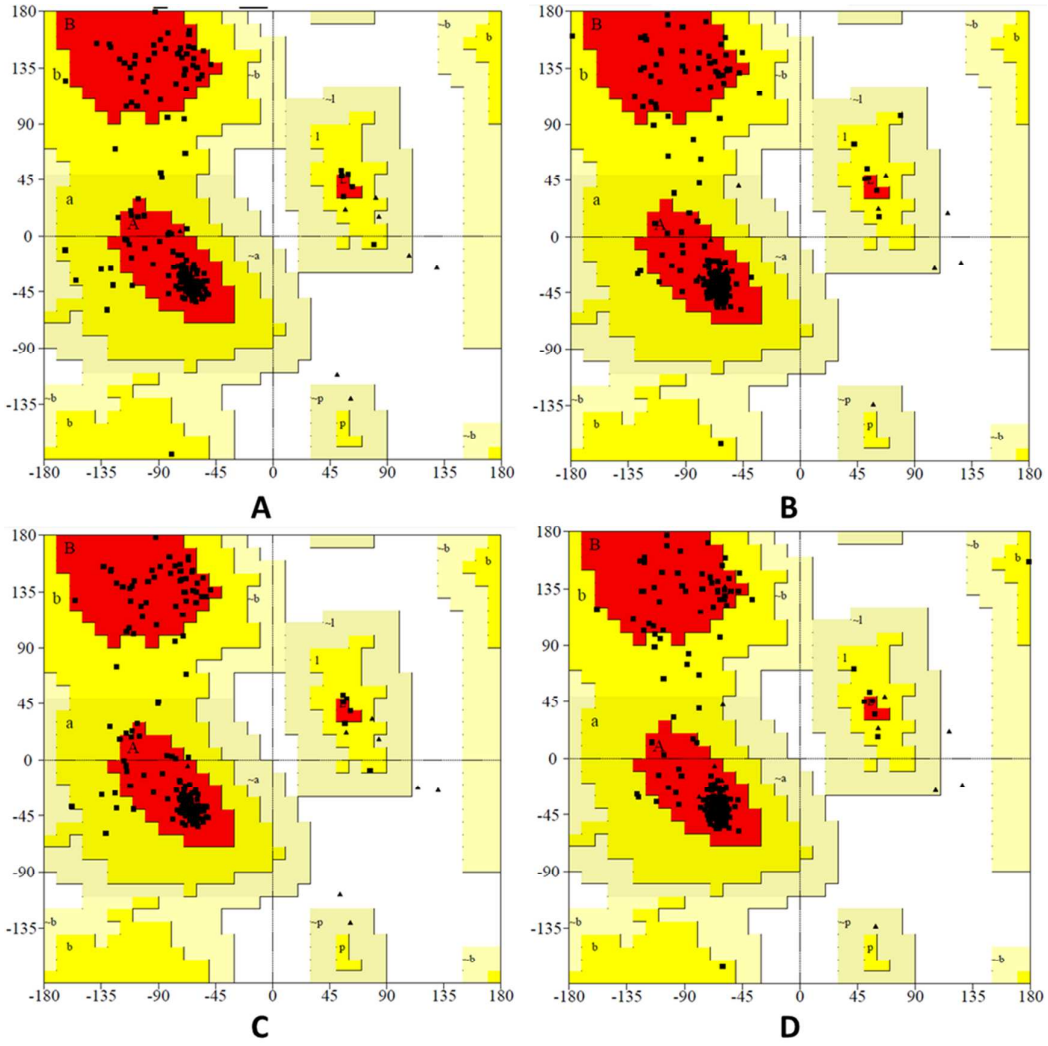

Figure S2. Ramachandran plot of built TR-LBD apo models. (A) Human TRα-LBD. (B) Human TRβ-LBD. (C) Rat TRα-LBD. (D) Rat TRβ-LBD. For each of the tested structures, more than 90% of residues were in most favored regions, and no residues were in generously allowed or disallowed regions.

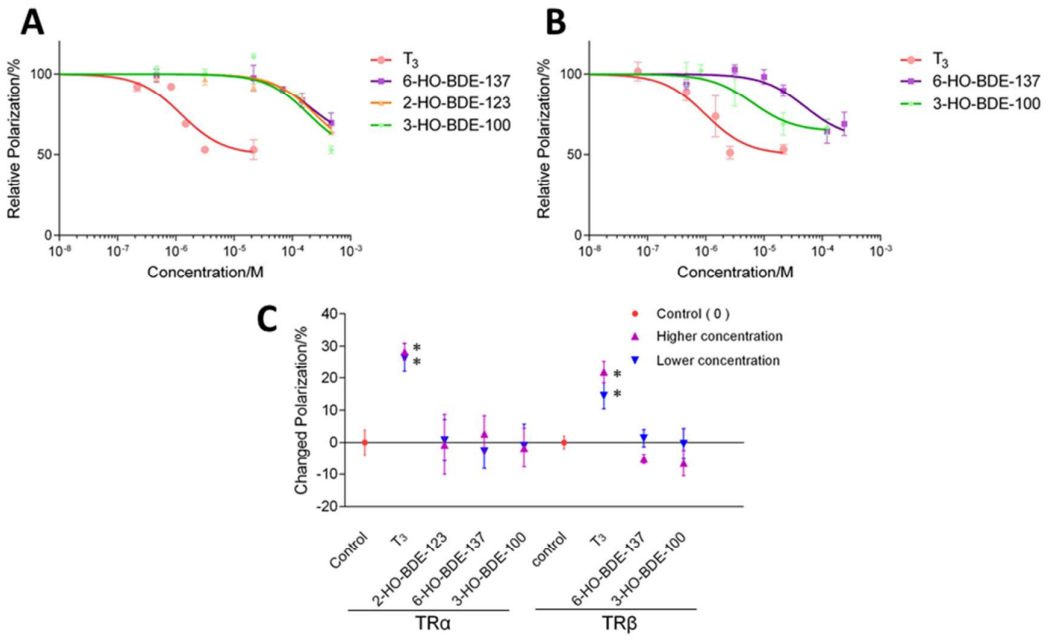

Figure S3. Results of competitive binding assays (A for TRα, B for TRβ) and coactivator recruitment assays (C). Relative polarization of solvent control is defined 100% in A and B. Higher concentration refers to 4.0×10^{-6}M for T_3, and 2.5×10^{-5}M for HO-PBDEs, and lower concentration refers to 1.0×10^{-6}M for T_3, and 1.0×10^{-5}M for HO-PBDEs. The error bar refers to the standard deviation (SD) of three independent experiments. * p<0.05 compared with solvent control.

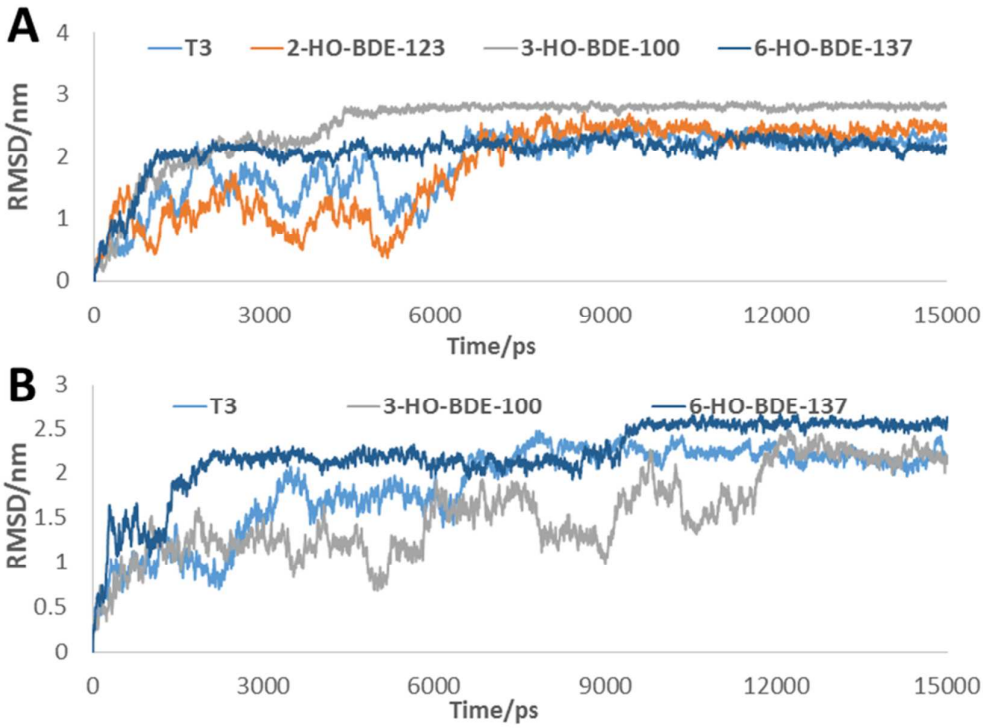

179

180 **Figure S4.** RMSDs for backbone atoms of H12 of human TRα (A) and TRβ (B).

181

182

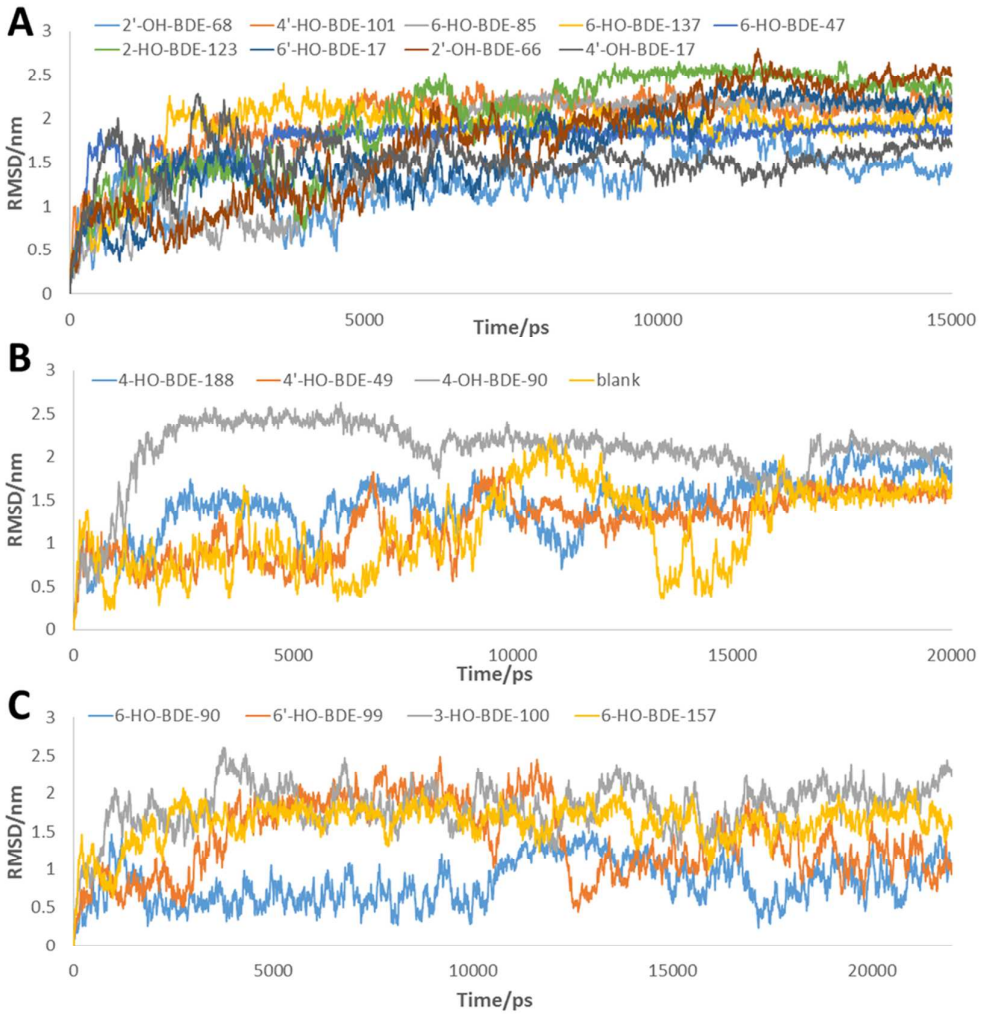
A
2'-OH-BDE-68
4'-HO-BDE-101
6-HO-BDE-85
6-HO-BDE-137
6-HO-BDE-47
2-HO-BDE-123
6'-HO-BDE-17
2'-OH-BDE-66
4'-OH-BDE-17
RMSD/nm
Time/ps
B
4-HO-BDE-188
4'-HO-BDE-49
4-OH-BDE-90
blank
RMSD/nm
Time/ps
C
6-HO-BDE-90
6'-HO-BDE-99
3-HO-BDE-100
6-HO-BDE-157
RMSD/nm
Time/ps

183

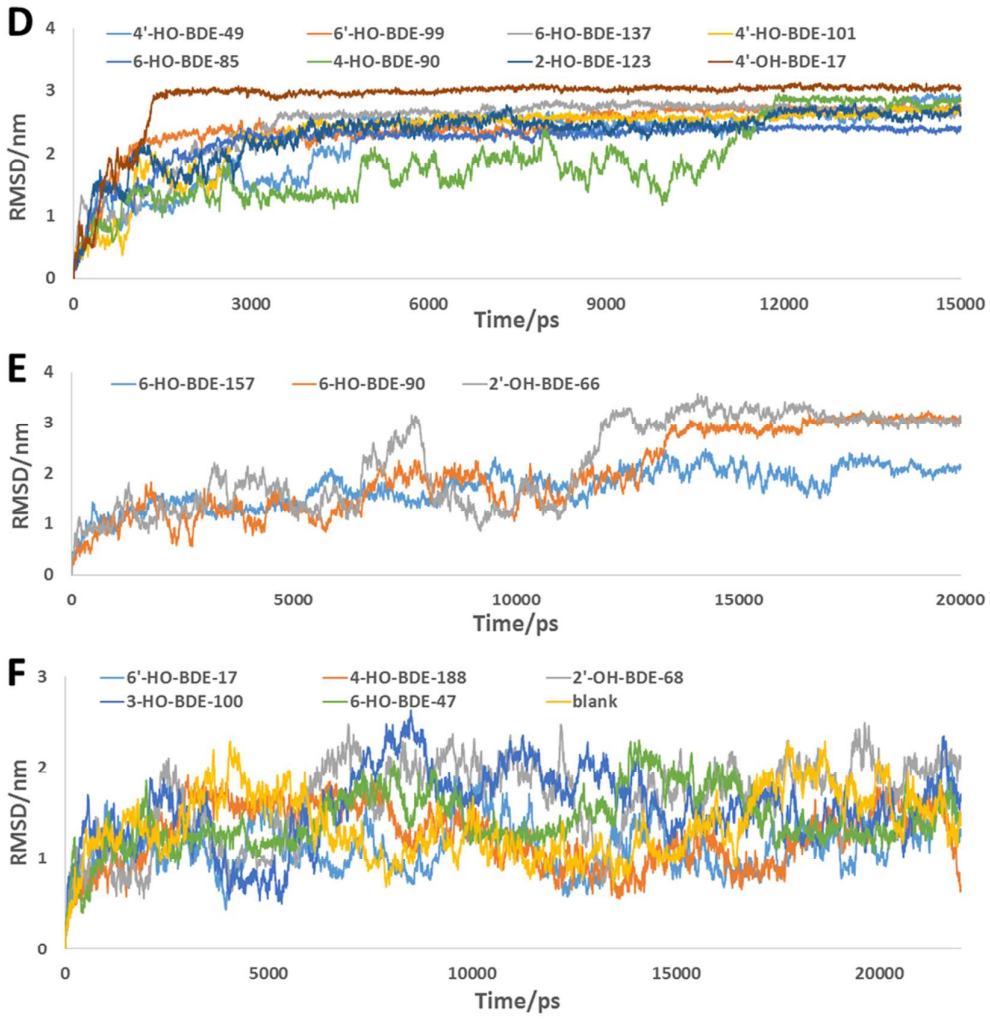

184

185 **Figure S5.** RMSD for backbone atoms of H12 of rat TRα (A, B and C) and TRβ (D, E and F).

186 Blank stands for H12 of unbound LBD.

187

188

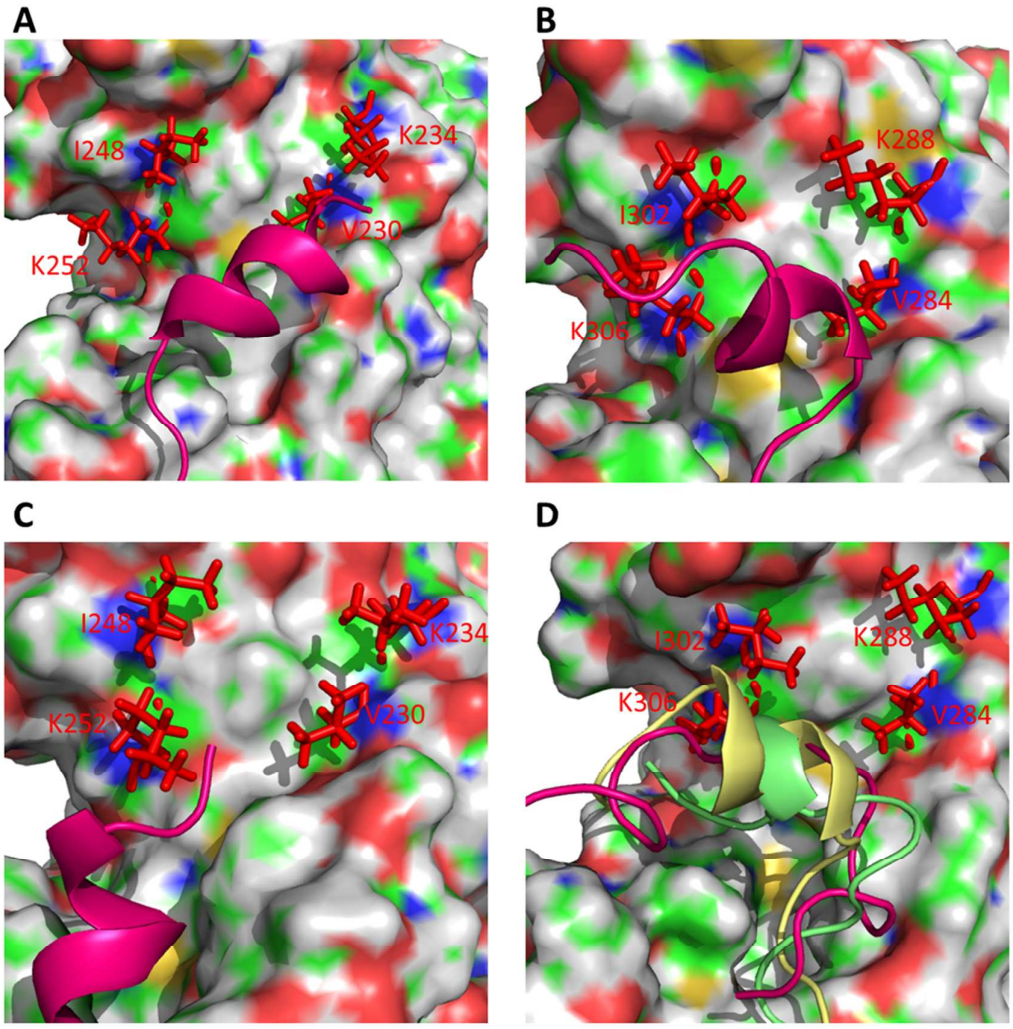

Figure S6. Equilibrated structures of ligand-bound conformations of human TRα/TRβ (A and B, respectively) and rat TRα/ TRβ (C and D, respectively). Main parts of the LBDs are shown as surface. Stable H12s of HO-PBDE-bound LBDs that inhibit binding of coactivators are shown as cartoon and colored hot pink (6-HO-BDE-85-bound, A; 2-HO-BDE-123-bound, B; 6-HO-BDE-85-bound, C; 2-HO-BDE-123-bound, D), lime (4-HO-BDE-90-bound, D) and pale yellow (6-HO-BDE-137, D). Residues V230, K234, I248 and K252 of TRα as well as V284, K288, I302 and K306 of TRβ, which are components of activation function 2 (AF-2), are labeled and colored red.

198

199

Reference

(1) Ren, X.; Guo, L.; Gao, Y.; Zhang, B.; Wan, B. Hydroxylated polybrominated diphenyl ethers exhibit different activities on thyroid hormone receptors depending on their degree of bromination. *Toxicol. Appl. Pharm.* **2013,** *268* (3), 256-263.

(2) Clark, M.; Cramer, R. D.; Van Opdenbosch, N. Validation of the general purpose Tripos 5.2 force field. *J. Comput. Chem.* **1989,** *10* (8), 982-1012.

(3) Biasini, M.; Bienert, S.; Waterhouse, A.; Arnold, K.; Studer, G.; Schmidt, T.; Kiefer, F.; Cassarino, T. G.; Bertoni, M.; Bordoli, L. SWISS-MODEL: modelling protein tertiary and quaternary structure using evolutionary information. *Nucleic. Acids. Res.* **2014**, *42* (1), 252-258.

(4) Arnold, K.; Bordoli, L.; Kopp, J.; Schwede, T. The SWISS-MODEL workspace: a web-based environment for protein structure homology modelling. *Bioinformatics.* **2006,** *22* (2), 195-201.

(5) Kiefer, F.; Arnold, K.; Künzli, M.; Bordoli, L.; Schwede, T. The SWISS-MODEL Repository and associated resources. *Nucleic. Acids. Res.* **2009,** *37* (suppl 1), D387-D392.

(6) Guex, N.; Peitsch, M. C.; Schwede, T. Automated comparative protein structure modeling with SWISS‐MODEL and Swiss‐PdbViewer: A historical perspective. *Electrophoresis.* **2009,** *30* (S1), S162-S173.

(7) Laskowski, R. A.; MacArthur, M. W.; Moss, D. S.; Thornton, J. M. PROCHECK: a program to check the stereochemical quality of protein structures. *J. Appl. Crystallogr.* **1993,** *26* (2), 283-291.

(8) Laskowski, R. A.; Rullmann, J. A. C.; MacArthur, M. W.; Kaptein, R.; Thornton, J. M. AQUA and PROCHECK-NMR: programs for checking the quality of protein structures solved by NMR. *J. Biomol. NMR.* **1996,** *8* (4), 477-486.

(9) Jain, A. N. Surflex-Dock 2.1: robust performance from ligand energetic modeling, ring flexibility, and knowledge-based search. *J. Comput. Aid. Mol. Des.* **2007,** *21* (5), 281-306.

(10) Karplus, M. CHARMM: A program for macromolecular energy, minimization, and dynamics calculations. *J. Comput. Chem.* **1983,** *4*, 187-217.

(11) MacKerell, A. D.; Bashford, D.; Bellott, M.; Dunbrack, R.; Evanseck, J.; Field, M. J.; Fischer, S.; Gao, J.; Guo, H.; Ha, S.; Joseph-McCarthy, D.; Kuchnir, L.; Kuczera, K.;Lau, F. T. K.; Mattos, C.; Michnick, S.; Ngo, T.; Nguyen, D. T.; Prodhom, B.; Reiher, W. E.; Roux, B.; Schlenkrich, M.; Smith, J. C.; Stote, R.; Straub, J.; Watanabe, M.; Wiórkiewicz-Kuczera, J.; Yin, D.; Karplus, M. All-atom empirical potential for molecular modeling and dynamics studies of proteins. *J. Phys. Chem. B.* **1998,** *102* (18), 3586-3616.

(12) Hess, B.; Kutzner, C.; Van Der Spoel, D.; Lindahl, E. GROMACS 4: algorithms for highly efficient, load-balanced, and scalable molecular simulation. *J. Chem. Theory. Comput.* **2008,** *4* (3), 435-447.

(13) Berendsen, H. J.; van der Spoel, D.; van Drunen, R. GROMACS: A message-passing parallel molecular dynamics implementation. *Comput. Phys. Commun.* **1995,** *91* (1), 43-56.

(14) Zoete, V.; Cuendet, M. A.; Grosdidier, A.; Michielin, O. SwissParam: a fast force field generation

tool for small organic molecules. *J. Comput. Chem.* **2011,** *32* (11), 2359-2368.

(15) Jorgensen, W. L.; Chandrasekhar, J.; Madura, J. D.; Impey, R. W.; Klein, M. L. Comparison of simple potential functions for simulating liquid water. *J. Chem. Phys.* **1983,** *79* (2), 926-935.

(16) Madauss, K. P.; Grygielko, E. T.; Deng, S.; Sulpizio, A. C.; Stanley, T. B.; Wu, C.; Short, S. A.; Thompson, S. K.; Stewart, E. L.; Laping, N. J. A structural and in vitro characterization of asoprisnil: a selective progesterone receptor modulator. *Mol. Endocrinol.* **2007,** *21* (5), 1066-1081.

(17) Marimuthu, A.; Feng, W.; Tagami, T.; Nguyen, H.; Jameson, J. L.; Fletterick, R. J.; Baxter, J. D.; West, B. L. TR surfaces and conformations required to bind nuclear receptor corepressor. *Mol. Endocrinol.* **2002,** *16* (2), 271-286.

(18) Hsieh, R. W.; Rajan, S. S.; Sharma, S. K.; Guo, Y.; DeSombre, E. R.; Mrksich, M.; Greene, G. L. Identification of ligands with bicyclic scaffolds provides insights into mechanisms of estrogen receptor subtype selectivity. *J. Biol. Chem.* **2006,** *281* (26), 17909-17919.

(19) Macindoe, G.; Mavridis, L.; Venkatraman, V.; Devignes, M.-D.; Ritchie, D. W. HexServer: an FFT-based protein docking server powered by graphics processors. *Nucleic. Acids. Res.* **2010**, *38* (S2), W445-W499.

(20) Kumari, R.; Kumar, R.; Lynn, A. g_mmpbsa: a GROMACS tool for high-throughput MM-PBSA calculations. *J. Chem. Inf. Model.* **2014,** *54* (7), 1951-1962.

(21) Baker, N. A.; Sept, D.; Joseph, S.; Holst, M. J.; McCammon, J. A. Electrostatics of nanosystems:

255 application to microtubules and the ribosome. *P. Nat. Acad. Sci.* **2001,** *98* (18), 10037-10041.

256